



REVIEW ARTICLE

# Instability of the peaked travelling wave in a local model for shallow water waves

Fabio Natali<sup>1</sup>, Dmitry E. Pelinovsky<sup>2</sup>  and Shuoyang Wang<sup>2</sup> 

<sup>1</sup>Departamento de Matemática, Universidade Estadual de Maringá, Avenida Colombo, CEP 87020-900, Maringá, PR, Brazil

<sup>2</sup>Department of Mathematics and Statistics, McMaster University, Hamilton, ON L8S 4K1, Canada

**Corresponding author:** Dmitry Pelinovsky; Email: [pelinod@mcmaster.ca](mailto:pelinod@mcmaster.ca)

**Keywords:** extended Hunter–Saxton equation; nonlinear stability; smooth and peaked profiles; spectral stability; traveling waves

(Received 25 February 2025; revised 8 July 2025; accepted 25 July 2025)

## Abstract

The travelling wave with the peaked profile is usually considered as a limit in the family of travelling waves with the smooth profiles. We study the linear and nonlinear stability of the peaked travelling wave by using a local model for shallow water waves, which is an extended version of the Hunter–Saxton equation. The evolution problem is well-defined in the function space  $H_{\text{per}}^1 \cap W^{1,\infty}$ , where we derive the linearised equations of motion and study the nonlinear evolution of co-periodic perturbations to the peaked periodic wave by using the method of characteristics. Within the linearised equations, we prove the spectral instability of the peaked travelling wave from the spectrum of the linearised operator in a Hilbert space, which completely covers the closed vertical strip with a specific half-width. Within the nonlinear equations, we prove the nonlinear instability of the peaked travelling wave by showing that the gradient of perturbations grows at the wave peak. By using numerical approximations of the smooth travelling waves and the spectrum of their associated linearised operator, we show that the spectral instability of the peaked travelling wave cannot be obtained as a limit in the family of the spectrally stable smooth travelling waves.

## 1. Introduction

Instabilities of steadily propagating waves with spatially periodic profiles on a fluid surface, called Stokes waves, have recently been explored within Euler’s equations in many computational details due to advanced numerical algorithms with high precision and accuracy [14–16, 28]. As the Stokes waves become steeper, they become increasingly unstable with respect to co-periodic perturbations, because the spectral stability problem admits more isolated unstable eigenvalues that bifurcate from the origin when pairs of purely imaginary eigenvalues coalesce and split into pairs of real eigenvalues [15, 28]. It is believed that the stability of the limiting Stokes waves with the peaked profile [3, 42, 44] can be concluded by studying eigenvalues of the spectral stability problem for the Stokes waves with the smooth profiles. A similar cascade of instabilities near the limit to the periodic wave with the maximal height is observed in other nonlocal wave models such as the Whitham equation [7].

The purpose of this paper is to study the linear and nonlinear instability of the travelling wave with a peaked profile within the following local model for the evolution of surface water waves:

$$2c\eta_{tx} = (c^2 - 2\eta)\eta_{xx} - (\eta_x)^2 + \eta, \quad (1.1)$$

where  $\eta = \eta(t, x)$  is the surface elevation and  $c > 0$  is the wave speed. The subscripts denote partial derivatives of  $\eta$  in  $t$  and  $x$ . We study  $2\pi$ -periodic solutions in  $x$  and denote the  $2\pi$ -periodic domain by  $\mathbb{T}$  so that  $\eta(t, x) : \mathbb{R} \times \mathbb{T} \rightarrow \mathbb{R}$ .

The local model (1.1) is an extended version of the Hunter–Saxton equation derived in [26] for the dynamics of direction fields. Indeed, if  $u = u(\tau, \xi)$  satisfies the Hunter–Saxton equation

$$(u_\tau + uu_\xi)_\xi = \frac{1}{2} (u_\xi)^2, \quad (1.2)$$

then the transformation

$$u(\tau, \xi) = 2\eta(t, x), \quad t = 2c\tau, \quad x = \xi + c^2\tau, \quad (1.3)$$

yields 1.1 without the last term.

The same model (1.1) was also discussed in [1, 2] in connection with the high-frequency limit of the Camassa–Holm equation, which is one of the toy models for fluid dynamics with smooth and peaked travelling waves:

$$u_\tau - u_{\tau\xi\xi} + ku_\xi + 3uu_\xi = 2u_\xi u_{\xi\xi} + uu_{\xi\xi\xi}, \quad (1.4)$$

where  $u = u(\tau, \xi)$  is the horizontal velocity and  $k > 0$  is the parameter. By using the transformation

$$u(\tau, \xi) = 2\eta(t, x), \quad t = 2c\varepsilon^{-1}\tau, \quad x = \varepsilon^{-1}(\xi - c^2\tau), \quad k = \varepsilon^{-2}, \quad (1.5)$$

keeping only the leading-order terms at the formal order of  $\mathcal{O}(\varepsilon^{-3})$ , and integrating in  $x$  with zero integration constant, we obtain (1.1) in the high-frequency limit  $\varepsilon \rightarrow 0$ .

The particular form of the local model (1.1) was suggested in [36] based on the reformulation of Euler's equations after a conformal transformation of the fluid domain with variable surface to a fixed rectangular domain and a formal truncation of the model near the travelling wave, see appendix A in [36]. In this context,  $x$  is the horizontal coordinate of the rectangular domain after the conformal transformation, and  $t$  is the time variable defined in the travelling frame moving with the speed  $c$ . As transformations (1.3) and (1.5) suggest, the factor  $2c$  in front of  $\eta_t$  in (1.1) can be removed by the scaling transformation. The travelling waves correspond to the time-independent solutions of the local model (1.1). The local model (1.1) represents the nonlocal Babenko equation [5] for travelling waves in shallow fluid after a transformation similar to the high-frequency limit (1.5) for the Camassa–Holm equation (1.4), see appendix B in [36].

Integrability of the local model (1.1) was established in [25] together with other peaked wave equations such as the reduced Ostrovsky and short-pulse equations. Some travelling wave solutions of these peaked wave equations were studied with Hirota's bilinear method in [40] and with dynamical system methods in [36]. Local well-posedness in Sobolev spaces for sufficiently smooth solutions has been proven in [45].

Both local models (1.1) and (1.4) have the travelling periodic waves with the smooth, peaked and cusped profiles such that the families of smooth and cusped profiles are connected at the limiting wave with the peaked profile [19, 34, 36]. In the Camassa–Holm equation (1.4), smooth travelling waves are linearly and nonlinearly stable [13, 17, 19, 31, 35, 38], whereas the peaked travelling waves are linearly and nonlinearly unstable in the  $W^{1,\infty}$  norm [30, 39, 41], despite the fact that the perturbations do not grow in the  $H^1$  norm [11, 12, 32, 33]. In the local model (1.1), the linear stability of the smooth periodic waves was proven in [36]. The linear and nonlinear instability of the limiting periodic wave with the peaked profile in  $H^1_{\text{per}} \cap W^{1,\infty}$  is the main result of the present study. Stability of the cusped travelling waves is an open problem for both models due to the lack of local well-posedness of the initial-value problem in the function spaces to which the cusped profiles belong.

For completeness, we also mention relevant results on the existence and stability of travelling periodic waves in the reduced Ostrovsky equation

$$(v_t + v v_x)_x = v, \quad (1.6)$$

which is very similar to the local model (1.1) rewritten in the form

$$(2c\eta_t - c^2\eta_x + 2\eta\eta_x)_x = \eta + (\eta_x)^2. \quad (1.7)$$

Linear and nonlinear stability of the smooth travelling periodic waves were obtained for the reduced Ostrovsky equation (1.6) in [20, 23, 27]. Uniqueness of the peaked travelling periodic waves was shown in [6, 21], where it was also shown that the cusped travelling periodic waves introduced in [24] by a coordinate transformation do not exist in the reduced Ostrovsky equation (1.6). The linear instability of the peaked travelling periodic wave was proven in [21, 22].

We note that the spectral stability problem  $L\psi = \lambda\psi'$  with a self-adjoint operator  $L$  in a Hilbert space, considered in [43], appears naturally for the linearisation of the nonlinear equation (1.7) at the smooth travelling periodic wave, with  $L$  being a Hessian operator defined by the variational characterisation of the travelling periodic waves, see (2.5) and (4.1) below. In the context of the reduced Ostrovsky equation (1.6), the same spectral stability problem  $L\psi = \lambda\psi'$  with a different Hessian operator  $L$  is obtained after the hodograph transformation [23, 24, 43].

In a similar context of the cubic Novikov equation, smooth travelling waves were found to be linearly and nonlinearly stable [18], whereas the peaked travelling waves were shown to be linearly and nonlinearly unstable in the  $W^{1,\infty}$  norm [10, 29] despite the perturbations do not grow in the  $H^1 \cap W^{1,4}$  norm [8, 9].

We now describe the main results and the organisation of the paper.

Section 2 presents the local well-posedness result in  $H^1_{\text{per}}(\mathbb{T}) \cap W^{1,\infty}(\mathbb{T})$  suitable for waves with the peaked profiles, see theorem 1 below, as well as the conserved quantities useful in the analysis of stability of travelling waves with both smooth and peaked profiles.

Section 3 introduces the travelling waves with the smooth and peaked profiles, see figure 1. Linearised equations of motion for the travelling waves are derived in section 4. For the smooth profiles, the spectral stability problem is equivalent to  $L\psi = \lambda\psi'$  with a self-adjoint operator  $L$  in a Hilbert space considered in [43], see equation (4.1). For the peaked profiles, the spectral stability problem  $L\psi = \lambda\psi'$  becomes singular and the proper linearisation is based on the local well-posedness result for the time evolution in  $H^1_{\text{per}}(\mathbb{T}) \cap W^{1,\infty}(\mathbb{T})$ , see equation (4.7). For the spectral theory in Hilbert spaces, it is more convenient to consider the linearised operator for the travelling wave with the peaked profile in the class of functions broader than the function space needed for the local well-posedness results. This gives us the linearised operator  $A : \mathcal{D} \subset L^2(\mathbb{T}) \rightarrow L^2(\mathbb{T})$  given by (4.14) and (4.15).

Sections 5 and 6 contain the spectral analysis of the linearised operator  $A : \mathcal{D} \subset L^2(\mathbb{T}) \rightarrow L^2(\mathbb{T})$  and its truncation to the unbounded local differential part  $A_0 : \mathcal{D} \subset L^2(\mathbb{T}) \rightarrow L^2(\mathbb{T})$ . In both cases, we obtain the exact location of the point spectrum and the resolvent set separated by the boundary, which belongs to the spectrum, see theorems 2 and 3 below. Since the spectrum is located in the closed vertical strip symmetrically with respect to  $i\mathbb{R}$  with a nonzero half-width of the strip, we conclude that the peaked travelling wave is spectrally unstable in a Hilbert space  $L^2(\mathbb{T})$ .

The nonlinear instability result for the peaked travelling wave is proven in section 7, see theorem 4, by using the method of characteristics. To define the nonlinear evolution and to use the method of characteristics, we again consider perturbations to the peaked travelling wave in the function space  $H^1_{\text{per}}(\mathbb{T}) \cap W^{1,\infty}(\mathbb{T})$ , which is a subset of the function space where the spectral instability has been proven. As a result, the nonlinear instability result is not trivially concluded from the spectral instability result. One of the main difficulties in establishing the nonlinear instability of the peaked travelling waves in the Hilbert space  $H^1_{\text{per}}(\mathbb{T})$  is that the initial-value problem associated with equation (1.7) cannot be solved using the semigroup approach for initial data in  $H^1_{\text{per}}(\mathbb{T})$ , compared to initial data in smoother

Sobolev spaces for the smooth travelling waves [45]. To prove the nonlinear instability of the peaked travelling wave, we show that the  $W^{1,\infty}$  norm of the perturbation grows in time. However, we do not know whether the  $H_{\text{per}}^1$  norm of the perturbation grows or remains bounded, in contrast to the case of the Camassa–Holm equation [12, 32].

Section 8 contains numerical approximations of the periodic waves with the smooth profiles and eigenvalues of the corresponding Hessian operator  $L$  in the spectral stability problem  $L\psi = \lambda\psi'$ . We show that the spectral instability of the peaked wave cannot be obtained as a limit in the family of the spectrally stable smooth waves. This further emphasises that the stability analysis of the smooth and peaked travelling waves is very different from each other.

## 2. Evolution and conserved quantities

Taking the mean value of the local model (1.7) for the  $C^1$ -smooth  $2\pi$ -periodic solutions  $\eta \in C^1(\mathbb{R} \times \mathbb{T})$  and integrating by parts yields the constraint

$$\oint [\eta + (\partial_x \eta)^2] dx = 0, \quad (2.1)$$

where  $\oint$  denotes the integral of a periodic function on  $\mathbb{T}$  over its period. The integral does not depend on the choice in the limits of integration.

Let  $\Pi_0 : L^2(\mathbb{T}) \rightarrow L^2(\mathbb{T})|_{\{1\}^\perp}$  be a projection operator to the periodic functions with zero mean. The local model (1.7) can be written in the evolution form

$$2c\partial_t \eta = (c^2 - 2\eta)\partial_x \eta + \Pi_0 \partial_x^{-1} \Pi_0 [(\partial_x \eta)^2 + \eta], \quad (2.2)$$

where  $\Pi_0 \partial_x^{-1} \Pi_0 : L^2(\mathbb{T}) \rightarrow L^2(\mathbb{T})|_{\{1\}^\perp}$  is uniquely defined on the periodic functions under the zero-mean constraint. The local well-posedness result suitable for solutions with peaked profiles is given by the following theorem.

**Theorem 1.** *For every  $\eta_0 \in H_{\text{per}}^1(\mathbb{T}) \cap W^{1,\infty}(\mathbb{T})$ , there exist  $\tau_0 > 0$  and a unique solution  $\eta \in C^0((-\tau_0, \tau_0), H_{\text{per}}^1(\mathbb{T}) \cap W^{1,\infty}(\mathbb{T})) \cap C^1((-\tau_0, \tau_0), L^2(\mathbb{T}) \cap L^\infty(\mathbb{T}))$  of the evolution equation (2.2) with  $\eta(0, \cdot) = \eta_0$ , which is also continuous with respect to the initial data  $\eta_0 \in H_{\text{per}}^1(\mathbb{T}) \cap W^{1,\infty}(\mathbb{T})$ .*

*Proof.* The evolution equation (2.2) is a nonlocal version of the inviscid Burgers equation  $2c\partial_t \eta = (c^2 - 2\eta)\partial_x \eta$ . Since

$$\begin{aligned} \|\Pi_0 \partial_x^{-1} \Pi_0 [\eta + (\partial_x \eta)^2]\|_{L^2} &\leq \|\eta + (\partial_x \eta)^2\|_{L^2} \leq \|\eta\|_{L^2} + \|\partial_x \eta\|_{L^\infty} \|\partial_x \eta\|_{L^2}, \\ \|\Pi_0 \partial_x^{-1} \Pi_0 [\eta + (\partial_x \eta)^2]\|_{L^\infty} &\leq \|\eta + (\partial_x \eta)^2\|_{L^1} \leq \sqrt{2\pi} \|\eta\|_{L^2} + \|\partial_x \eta\|_{L^2}^2, \\ \|\partial_x \Pi_0 \partial_x^{-1} \Pi_0 [\eta + (\partial_x \eta)^2]\|_{L^2 \cap L^\infty} &\leq \|\eta + (\partial_x \eta)^2\|_{L^2 \cap L^\infty} \leq \|\eta\|_{L^2 \cap L^\infty} + \|\partial_x \eta\|_{L^\infty} \|\partial_x \eta\|_{L^2 \cap L^\infty}, \end{aligned}$$

the nonlocal term  $\Pi_0 \partial_x^{-1} \Pi_0 [\eta + (\partial_x \eta)^2]$  is a bounded operator from a ball in  $H_{\text{per}}^1(\mathbb{T}) \cap W^{1,\infty}(\mathbb{T})$  to  $H_{\text{per}}^1(\mathbb{T}) \cap W^{1,\infty}(\mathbb{T})$ . Local well-posedness in  $H_{\text{per}}^1(\mathbb{T}) \cap W^{1,\infty}(\mathbb{T})$  follows by using the method of characteristics.  $\square$

**Remark 1.** The same argument can be used to establish the local well-posedness of the evolution equation (2.2) in smooth Sobolev spaces  $H_{\text{per}}^s(\mathbb{T})$  with  $s > \frac{3}{2}$ , see [45]. The smooth Sobolev spaces are continuously embedded into the function space  $H_{\text{per}}^1(\mathbb{T}) \cap W^{1,\infty}(\mathbb{T})$ .

The mass, momentum and energy conservation of the evolution equation (2.2) are obtained for the smooth solution  $\eta \in C^0((-\tau_0, \tau_0), H_{\text{per}}^s(\mathbb{T}))$  with  $s > \frac{3}{2}$ . Multiplying (1.1) by  $\partial_x \eta$ , and integrating over

the period, yields conservation of the momentum

$$Q(\eta) := \frac{1}{2} \oint (\partial_x \eta)^2 dx, \quad (2.3)$$

and in view of the constraint (2.1), also conservation of the mass

$$M(\eta) := \oint \eta dx. \quad (2.4)$$

Furthermore, writing (2.2) in the Hamiltonian form

$$2c\partial_t \eta = -\Pi_0 \partial_x^{-1} \Pi_0 [c^2 Q'(\eta) - H'(\eta)], \quad (2.5)$$

where

$$H(\eta) := \frac{1}{2} \oint [\eta^2 + 2\eta(\partial_x \eta)^2] dx, \quad (2.6)$$

yields conservation of the energy  $H(\eta)$ .

**Remark 2.** Due to the integrability of the local model (1.1), higher-order conserved quantities exist. Nevertheless, conservation of  $Q(\eta)$ ,  $M(\eta)$  and  $H(\eta)$  is sufficient for the existence and stability analysis of the travelling waves with the smooth and peaked profiles.

### 3. Travelling wave with the smooth and peaked profiles

A travelling wave with the speed  $c$  and the smooth profile  $\eta \in C_{\text{per}}^\infty(\mathbb{T})$  corresponds to the time-independent solution of the local model (1.1) found from the second-order differential equation

$$(c^2 - 2\eta)\eta'' - (\eta')^2 + \eta = 0, \quad x \in \mathbb{T}. \quad (3.1)$$

This equation is integrable with the first-order invariant

$$E(\eta, \eta') = \frac{1}{2}(c^2 - 2\eta)(\eta')^2 + \frac{1}{2}\eta^2 = \mathcal{E}, \quad (3.2)$$

the value of which is independent of  $x$ .

It was shown in [36] that the family of smooth  $2\pi$ -periodic solutions  $\eta \in C_{\text{per}}^\infty(\mathbb{T})$  exists for  $c \in (1, c_*)$  with  $c_* := \frac{\pi}{2\sqrt{2}}$ . The peaked profile  $\eta_* \in C_{\text{per}}^0(\mathbb{T}) \cap W^{1,\infty}(\mathbb{T})$  corresponds to  $c = c_*$  and is given explicitly as

$$\eta_*(x) = \frac{1}{16}(\pi^2 - 4\pi|x| + 2x^2), \quad x \in [-\pi, \pi], \quad (3.3)$$

extended as a  $2\pi$ -periodic function on  $\mathbb{T}$ . It is easy to verify the validity of  $\eta_*$  in (3.3) as a solution of (3.1) for  $x \in [-\pi, 0) \cup (0, \pi]$  with

$$\max_{x \in \mathbb{T}} \eta_*(x) = \eta_*(0) = \frac{c_*^2}{2}.$$

The peaked profile  $\eta_* \in C_{\text{per}}^0(\mathbb{T}) \cap W^{1,\infty}(\mathbb{T})$  corresponds to the marginal value of  $\mathcal{E}_c := \frac{c^4}{8}$  in (3.2), which separates the smooth profiles for  $\mathcal{E} \in (0, \mathcal{E}_c)$  and the cusped profiles for  $\mathcal{E} \in (\mathcal{E}_c, \infty)$ . The value

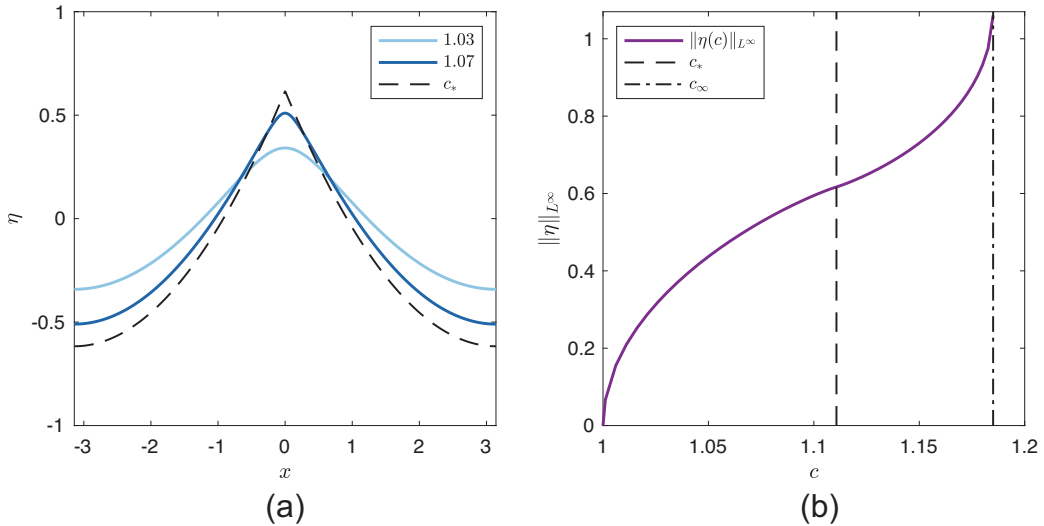


**Figure 1.** (a) The solid lines represent the smooth profiles  $\eta$  for  $c = 1.03, 1.07$ . The dashed line represents the peaked profile  $\eta_*$  for  $c = c_*$ . (b) The wave amplitude versus the wave speed  $c$  for smooth profiles in  $(1, c_*)$  and cusped profiles in  $(c_*, c_\infty)$ , where  $c_* \approx 1.1107$  (dashed line) and  $c_\infty \approx 1.1850$  (dashed-dotted line).

of  $c = c_*$  is selected by setting the period of the peaked profile to  $2\pi$ . The slope of the peaked profile  $\eta_*$  has a finite jump discontinuity at  $x = 0$  since

$$\eta'_*(x) = -\frac{1}{4}(\pi - |x|)\text{sign}(x) \quad x \in [-\pi, \pi], \quad (3.4)$$

which implies that  $\eta'_*(0^+) - \eta'_*(0^-) = -\frac{\pi}{2}$ . By using the Dirac delta distribution  $\delta_0$  at  $x = 0$ , we can express the finite jump discontinuity of  $\eta'_*(x)$  as the Dirac delta singularity of the second derivative at  $x = 0$ :

$$\eta''_*(x) = \frac{1}{4} - \frac{\pi}{2}\delta_0, \quad x \in [-\pi, \pi]. \quad (3.5)$$

It can be checked through explicit computations that the periodic solution with the peaked profile (3.3) satisfies the constraint (2.1).

Figure 1 presents the periodic profiles  $\eta$  of the travelling waves for two values of  $c$  in  $(1, c_*)$  and for  $c = c_*$  (left) as well as the dependence of the wave amplitude  $\|\eta\|_{L^\infty}$  versus  $c$  (right). The wave profiles were approximated numerically, see section 8. The peaked profile  $\eta_*$  is shown by a dashed line on the left panel, and the corresponding value  $c_*$  is shown by a dashed vertical line on the right panel. The family of periodic waves is continued past  $c = c_*$  with the cusped profiles for  $c \in (c_*, c_\infty)$  which satisfy

$$\eta(x) = \frac{c^2}{2} - A(c)|x|^{2/3} + \mathcal{O}(|x|), \quad \text{as } |x| \rightarrow 0, \quad (3.6)$$

where  $A(c) > 0$  is a numerical coefficient and the value of  $c_\infty$  is numerically computed (dashed-dotted line on figure 1) [36].

**Remark 3.** In the context of Babenko's equation [5] for the fluid of infinite depth, it is shown in [37] that the peaked profiles with the local behaviour as in (3.4) do not exist after the conformal transformation

of the fluid domain, whereas the cusped profiles satisfying (3.6) in the conformal coordinate correspond to the limiting Stokes waves with a 120-degree crest angle in the original spatial coordinate. We make no claims that the peaked behaviour of the toy model (1.1) corresponds to the limiting Stokes wave of the original Euler's equations.

#### 4. Linearisation at the smooth and peaked travelling waves

Let  $\eta \in C_{\text{per}}^\infty(\mathbb{T})$  be the spatial profile of the smooth travelling waves for  $c \in (1, c_*)$ . The second-order equation (3.1) is equivalent to the Euler–Lagrange equation

$$H'(\eta) - c^2 Q'(\eta) = 0.$$

Adding a perturbation  $\zeta(t, x)$  to  $\eta(x)$  and linearising the evolution equation (2.5), we obtain the linearised equation in the form

$$2c\partial_t \zeta = -\Pi_0 \partial_x^{-1} \Pi_0 \mathcal{L} \zeta, \quad \mathcal{L} := -\partial_x (c^2 - 2\eta) \partial_x + (2\eta'' - 1), \quad (4.1)$$

where  $\mathcal{L} : H_{\text{per}}^2(\mathbb{T}) \subset L^2(\mathbb{T}) \rightarrow L^2(\mathbb{T})$  is the Hessian operator for  $c^2 Q(\eta) - H(\eta)$  at the profile  $\eta \in C_{\text{per}}^\infty(\mathbb{T})$ . As  $c \rightarrow c_*$  and  $\eta \rightarrow \eta_* \in C_{\text{per}}^0(\mathbb{T}) \cap W^{1,\infty}(\mathbb{T})$ , the Hessian operator becomes singular since

$$2\eta_*''(x) - 1 = -\frac{1}{2} - \pi\delta_0, \quad x \in [-\pi, \pi].$$

This suggests that the linearised equation (4.1) defined along the family of the smooth travelling waves breaks at the peaked travelling wave. We need to be careful to linearise the evolution equation (2.5) about the travelling wave with the peaked profile  $\eta_*$  by working in the function space  $H_{\text{per}}^1(\mathbb{T}) \cap W^{1,\infty}(\mathbb{T})$ , where the local well-posedness is established by theorem 1.

To get the proper linearisation near the peaked profile  $\eta_*$ , we note the following result, which is obtained verbatim from the analysis of [39, 41].

**Lemma 1.** [39, 41] *Consider a local solution  $\eta \in C^0((-\tau_0, \tau_0), H_{\text{per}}^1(\mathbb{T}) \cap W^{1,\infty}(\mathbb{T}))$  of theorem 1, and assume that there exists  $\xi(t)$  such that*

$$\lim_{x \rightarrow \xi(t)^-} \partial_x \eta(t, x) \neq \lim_{x \rightarrow \xi(t)^+} \partial_x \eta(t, x), \quad t \in (-\tau_0, \tau_0).$$

*Then,  $\xi \in C^1((-\tau_0, \tau_0))$  satisfies*

$$\xi'(t) = -\frac{1}{2c} (c^2 - 2\eta(t, \xi(t))), \quad t \in (-\tau_0, \tau_0). \quad (4.2)$$

In order to consider a local solution  $\eta \in C^0((-\tau_0, \tau_0), H_{\text{per}}^1(\mathbb{T}) \cap W^{1,\infty}(\mathbb{T}))$  of the evolution equation (2.2) in a local neighbourhood of the travelling wave with the peaked profile (3.3), we define the decomposition

$$\eta(t, x) = \eta_*(x - \xi(t)) + \zeta(t, x - \xi(t)), \quad (4.3)$$

where we assume that the only peak of  $\eta(t, \cdot)$  on  $\mathbb{T}$  is located at  $x = \xi(t)$  for some  $t \in (-\tau_0, \tau_0)$ . The peak location  $\xi(t)$  moves with the local characteristic speed of the inviscid Burgers equation, as in Lemma 1. Substituting (4.3) into (2.2) with  $c = c_*$  and using (4.2) yields the evolution problem for the perturbation

term  $\zeta(t, x)$ :

$$2c_*\partial_t\zeta = (c_*^2 - 2\eta_*)\partial_x\zeta - 2(\zeta - \zeta|_{x=0})(\eta'_* + \partial_x\zeta) + \Pi_0\partial_x^{-1}\Pi_0[\zeta + 2\eta'_*\partial_x\zeta + (\partial_x\zeta)^2], \quad (4.4)$$

where we have translated  $x - \xi(t)$  into  $x$  on  $\mathbb{T}$ . Truncation of the evolution equation (4.4) by the linear terms in  $\zeta$  yields the linearised equation

$$2c_*\partial_t\zeta = (c_*^2 - 2\eta_*)\partial_x\zeta - 2\eta'_*(\zeta - \zeta|_{x=0}) + \Pi_0\partial_x^{-1}\Pi_0[\zeta + 2\eta'_*\partial_x\zeta], \quad (4.5)$$

subject to the linearised constraint

$$\oint [\zeta + 2\eta'_*\partial_x\zeta]dx = 0. \quad (4.6)$$

The next result gives the equivalent form of the linearised evolution.

**Lemma 2.** *The linearised equation (4.5) is equivalently written in the form*

$$2c_*\partial_t\zeta = (c_*^2 - 2\eta_*)\partial_x\zeta - \frac{1}{\pi}\oint \eta'_*\zeta dx + \frac{1}{2}\Pi_0\partial_x^{-1}\Pi_0\zeta, \quad (4.7)$$

where both  $\oint \zeta dx$  and  $\zeta|_{x=0}$  are constant in  $t$  and satisfies the constraint

$$\zeta|_{x=0} = -\frac{1}{2\pi}\oint \zeta dx, \quad (4.8)$$

*Proof.* The constraint (4.8) is obtained by substituting (3.4) into (4.6), and integrating the second term in (4.6) by parts. To simplify the linearised equation (4.5), we use (3.5) and write

$$\zeta + 2\eta'_*\partial_x\zeta = 2\partial_x(\eta'_*\zeta) + \frac{1}{2}\zeta + \pi\delta_0\zeta. \quad (4.9)$$

This transforms the linearised equation (4.5) to the form

$$2c_*\partial_t\zeta = (c_*^2 - 2\eta_*)\partial_x\zeta - \frac{1}{\pi}\oint \eta'_*\zeta dx + 2\eta'_*\zeta|_{x=0} + \frac{1}{2}\Pi_0\partial_x^{-1}\Pi_0\zeta + \pi\zeta|_{x=0}\Pi_0\partial_x^{-1}\Pi_0\delta_0. \quad (4.10)$$

By using Fourier series, we get

$$\delta_0 = \frac{1}{2\pi} \sum_{n \in \mathbb{Z}} e^{inx},$$

so that

$$\Pi_0\partial_x^{-1}\Pi_0\delta_0 = \Pi_0\partial_x^{-1}\left(\delta_0 - \frac{1}{2\pi}\right) = \sum_{n \in \mathbb{Z} \setminus \{0\}} \frac{1}{2\pi in} e^{inx}.$$

On the other hand, it follows from (3.5) that

$$\eta''_*(x) = \frac{1}{4} - \frac{\pi}{2}\delta_0 = -\frac{1}{4} \sum_{n \in \mathbb{Z} \setminus \{0\}} e^{inx},$$



which yields

$$\eta'_*(x) = - \sum_{n \in \mathbb{Z} \setminus \{0\}} \frac{1}{4in} e^{inx}.$$

Hence, the two terms with  $\zeta|_{x=0}$  in (4.10) cancels out as

$$2\eta'_* + \pi \Pi_0 \partial_x^{-1} \Pi_0 \delta_0 = 0, \quad (4.11)$$

and the linearised equation (4.10) can be written in the form (4.7).

Finally, we show that both  $\oint \zeta dx$  and  $\zeta|_{x=0}$  are constant in  $t$ . The conservation of  $\oint \zeta dx$  follows by taking the mean value of (4.7), with the account of the projection term  $-\frac{1}{\pi} \oint \eta'_* \zeta dx$ . The conservation of  $\zeta|_{x=0}$  is shown by taking the limit  $x \rightarrow 0$  since if  $\zeta = \sum_{n \in \mathbb{Z}} \zeta_n e^{inx}$ , then

$$\begin{aligned} \frac{1}{\pi} \oint \eta'_* \zeta dx &= \frac{1}{\pi} \sum_{n \in \mathbb{Z} \setminus \{0\}} \zeta_n \oint \eta'_*(x) e^{inx} dx \\ &= -\frac{1}{\pi} \sum_{n \in \mathbb{Z} \setminus \{0\}} \zeta_n \left( \sum_{m \in \mathbb{Z} \setminus \{0\}} \frac{1}{4im} \oint e^{i(n+m)x} dx \right) \\ &= \sum_{n \in \mathbb{Z} \setminus \{0\}} \frac{\zeta_n}{2in} \end{aligned} \quad (4.12)$$

and

$$\lim_{x \rightarrow 0} \frac{1}{2} \Pi_0 \partial_x^{-1} \Pi_0 \zeta = \lim_{x \rightarrow 0} \frac{1}{2} \sum_{n \in \mathbb{Z} \setminus \{0\}} \zeta_n \Pi_0 \partial_x^{-1} e^{inx} = \sum_{n \in \mathbb{Z} \setminus \{0\}} \frac{\zeta_n}{2in}, \quad (4.13)$$

from which it follow that  $2c \lim_{x \rightarrow 0} \partial_t \zeta(t, x) = 0$  and the value of  $\zeta|_{x=0}$  is preserved in time.  $\square$

The linearised equation (4.7) of lemma 2 is defined by the linearised operator  $A : \text{Dom}(A) \subset L^2(\mathbb{T}) \rightarrow L^2(\mathbb{T})$  given by

$$Af := (c_*^2 - 2\eta_*) \partial_x f - \frac{1}{\pi} \oint \eta'_* f dx + \frac{1}{2} \Pi_0 \partial_x^{-1} \Pi_0 f, \quad (4.14)$$

where

$$\text{Dom}(A) := \{f \in L^2(\mathbb{T}) : (c_*^2 - 2\eta_*) f' \in L^2(\mathbb{T})\} \equiv \mathcal{D}. \quad (4.15)$$

**Remark 4.** The local well-posedness result of Theorem 1 suggests that we should consider the linear operator  $A : H_{\text{per}}^1(\mathbb{T}) \cap W^{1,\infty}(\mathbb{T}) \subset L^2(\mathbb{T}) \cap L^\infty(\mathbb{T}) \rightarrow L^2(\mathbb{T}) \cap L^\infty(\mathbb{T})$  with the same definition of  $A$  as in (4.14). However, for the spectral stability theory, it is more convenient to work in a Hilbert space  $L^2(\mathbb{T})$  for which the domain of  $A$  is given by (4.15).

We denote the spectrum of  $A : \mathcal{D} \subset L^2(\mathbb{T}) \rightarrow L^2(\mathbb{T})$  by  $\sigma(A)$ . According to the standard definition (definition 6.1.9 in [4]), the spectrum  $\sigma(A)$  is further divided into three disjoint sets of the point spectrum  $\sigma_p(A)$ , the residual spectrum  $\sigma_r(A)$ , and the continuous spectrum  $\sigma_c(A)$  with the resolvent set denoted by  $\rho(A) = \mathbb{C} \setminus \sigma(A)$ .

**Remark 5.** By using (2.1), (3.4) and (3.5), as well as  $c_* = \frac{\pi}{2\sqrt{2}}$ , we obtain

$$\begin{aligned} A\eta'_* &= (c_*^2 - 2\eta_*)\eta''_* - \frac{1}{\pi} \oint (\eta'_*)^2 dx + \frac{1}{2}\Pi_0\eta_* \\ &= -\frac{\pi}{2}(c_*^2 - 2\eta_*)\delta_0 + \frac{1}{4}(c_*^2 - 2\eta_*) - \frac{1}{\pi} \oint (\eta'_*)^2 dx + \frac{1}{2}\eta_* - \frac{1}{4\pi} \oint \eta_* dx \\ &= -\frac{\pi}{2}(c_*^2 - 2\eta_*)\delta_0 + \frac{\pi^2}{32} - \frac{3}{4\pi} \oint (\eta'_*)^2 dx \\ &= -\frac{\pi}{2}(c_*^2 - 2\eta_*)\delta_0, \end{aligned}$$

so that  $A\eta'_* = 0$  in  $L^2(\mathbb{T})$ . Similarly, we have  $\eta'_* \in \mathcal{D}$  so that  $0 \in \sigma_p(A)$ . However,  $\eta'_* \notin C_{\text{per}}^0(\mathbb{T})$ , hence  $\eta'_* \notin H_{\text{per}}^1(\mathbb{T}) \cap W^{1,\infty}(\mathbb{T})$ . Thus,  $H_{\text{per}}^1(\mathbb{T}) \cap W^{1,\infty}(\mathbb{T})$  is embedded into  $\mathcal{D}$  but is not equivalent to  $\mathcal{D}$ . The spectral theory of the linear operator  $A : \mathcal{D} \subset L^2(\mathbb{T}) \rightarrow L^2(\mathbb{T})$  is developed in a wider space of functions than the space needed for the local well-posedness of the evolution equation (2.2).

## 5. Truncated linearised equation

The following lemma allows us to truncate the linearised operator (4.14) and (4.15).

**Lemma 3.** *The linear operator  $K := \frac{1}{2}\Pi_0\partial_x^{-1}\Pi_0 : L^2(\mathbb{T}) \rightarrow L^2(\mathbb{T})$  is a compact (Hilbert–Schmidt) operator.*

*Proof.* By the Fourier theory, we have

$$\sigma(K) = \sigma_p(K) = \left\{ \frac{1}{2n}, \quad n \in \mathbb{Z} \setminus \{0\} \right\}.$$

Since eigenvalues of  $\sigma_p(K)$  are square summable,  $K : L^2(\mathbb{T}) \rightarrow L^2(\mathbb{T})$  is a compact (Hilbert–Schmidt) operator.  $\square$

Using lemma 3, we see that  $A = A_0 + K$ , where  $K$  is a compact perturbation of the unbounded truncated operator  $A_0 : \text{Dom}(A_0) \subset L^2(\mathbb{T}) \rightarrow L^2(\mathbb{T})$  given by

$$A_0 f := (c_*^2 - 2\eta_*)\partial_x f - \frac{1}{\pi} \oint \eta'_*(x)f(x)dx, \quad (5.1)$$

with the same  $\text{Dom}(A_0) = \text{Dom}(A) = \mathcal{D}$ . The constraint in the definition of  $A_0$  ensures that

$$\oint (A_0 f)(x)dx = 0 \quad \text{if } f \in \mathcal{D}. \quad (5.2)$$

The spectrum of  $A_0$  can be analysed similarly to the work [22]. In fact, since

$$c_*^2 - 2\eta_*(x) = \frac{1}{4}[\pi^2 - (\pi - |x|)^2], \quad x \in [-\pi, \pi],$$

extended as a  $2\pi$ -periodic function on  $\mathbb{T}$ , we define the change of coordinates  $x \mapsto z$  by

$$\frac{dx}{dz} = \frac{1}{4}x(2\pi - x), \quad x \in [0, 2\pi], \quad (5.3)$$

where the interval  $[0, 2\pi]$  is located between the two consequent peaks on the periodic domain  $\mathbb{T}$ . Solving the differential equation (5.3) with  $x(0) = \pi$  yields

$$x(z) = \pi + \pi \tanh\left(\frac{\pi z}{4}\right), \quad (5.4)$$

which is an invertible mapping  $\mathbb{R} \ni z \mapsto x \in [0, 2\pi]$ . The following lemma shows that the spectrum of the operator  $A_0 : \mathcal{D} \subset L^2(\mathbb{T}) \rightarrow L^2(\mathbb{T})$  can be found from the spectrum of a simpler linear operator defined on the infinite line  $\mathbb{R}$ .

**Lemma 4.** *The spectrum of the truncated operator  $A_0 : \mathcal{D} \subset L^2(\mathbb{T}) \rightarrow L^2(\mathbb{T})$  coincides with the spectrum of the linear operator  $D_0 : H^1(\mathbb{R}) \subset L^2(\mathbb{R}) \rightarrow L^2(\mathbb{R})$  given by*

$$D_0 h := \partial_z h + \frac{\pi}{4} \tanh\left(\frac{\pi z}{4}\right) h + \frac{\pi}{4} w(z) \int_{\mathbb{R}} w'(z) h(z) dz, \quad (5.5)$$

where  $w(z) := \operatorname{sech}\left(\frac{\pi z}{4}\right)$ . The constraint (5.2) coincides with the constraint  $\langle w, D_0 h \rangle = 0$ , which holds for every  $h \in H^1(\mathbb{R})$ , where  $\langle \cdot, \cdot \rangle$  is the standard inner product in  $L^2(\mathbb{R})$  with the induced norm  $\|\cdot\|$ .

*Proof.* Using the transformation (5.4), we obtain  $A_0 f = B_0 g$ , where  $g(z) = f(x)$  and  $B_0 : \operatorname{Dom}(B_0) \subset L_w^2(\mathbb{R}) \rightarrow L_w^2(\mathbb{R})$  is given by

$$B_0 g := \partial_z g + \frac{\pi}{4} \int_{\mathbb{R}} w(z) w'(z) g(z) dz \quad (5.6)$$

and

$$\operatorname{Dom}(B_0) := \{g \in L_w^2(\mathbb{R}) : g' \in L_w^2(\mathbb{R})\} \equiv H_w^1(\mathbb{R}),$$

with the weight  $w(z) := \operatorname{sech}\left(\frac{\pi z}{4}\right)$ . Here the exponentially weighted spaces  $L_w^2(\mathbb{R})$  and  $H_w^1(\mathbb{R})$  are defined with the squared norms:

$$\|g\|_{L_w^2}^2 = \int_{\mathbb{R}} w^2(z) |g(z)|^2 dz, \quad \|g\|_{H_w^1}^2 = \int_{\mathbb{R}} w^2(z) \left( |g'(z)|^2 + |g(z)|^2 \right) dz$$

and the inner product in  $L_w^2(\mathbb{R})$  is defined by

$$\langle g_1, g_2 \rangle_{L_w^2} = \int_{\mathbb{R}} w^2(z) g_1(z) g_2(z) dz.$$

The constraint (5.2) coincides with the constraint  $\langle 1, B_0 g \rangle_{L_w^2} = 0$ , which holds for every  $g \in H_w^1(\mathbb{R})$ . By using the change of variables  $h(z) = w(z)g(z)$ , we get  $B_0 g = w^{-1} D_0 h$  and  $\langle 1, B_0 g \rangle_{L_w^2} = \langle w, D_0 h \rangle = 0$ , where  $D_0 : H^1(\mathbb{R}) \subset L^2(\mathbb{R}) \rightarrow L^2(\mathbb{R})$  is given by (5.5). Due to the transformations above, the spectrum of  $A_0 : \mathcal{D} \subset L^2(\mathbb{T}) \rightarrow L^2(\mathbb{T})$  coincides with the spectrum of the linear operator  $D_0 : H^1(\mathbb{R}) \subset L^2(\mathbb{R}) \rightarrow L^2(\mathbb{R})$ .  $\square$

The following theorem prescribes the spectrum of the truncated operator  $A_0 : \mathcal{D} \subset L^2(\mathbb{T}) \rightarrow L^2(\mathbb{T})$  given by (5.1).

**Theorem 2.** *The spectrum of  $A_0 : \mathcal{D} \subset L^2(\mathbb{T}) \rightarrow L^2(\mathbb{T})$  completely covers the closed vertical strip given by*

$$\sigma(A_0) = \left\{ \lambda \in \mathbb{C} : -\frac{\pi}{4} \leq \operatorname{Re}(\lambda) \leq \frac{\pi}{4} \right\}. \quad (5.7)$$

*Proof.* We obtain  $\sigma_p(A_0)$  and  $\rho(A_0)$  as

$$\sigma_p(A_0) = \left\{ \lambda \in \mathbb{C} : -\frac{\pi}{4} < \operatorname{Re}(\lambda) < \frac{\pi}{4} \right\}, \quad (5.8)$$

$$\rho(A_0) = \left\{ \lambda \in \mathbb{C} : |\operatorname{Re}(\lambda)| > \frac{\pi}{4} \right\}. \quad (5.9)$$

Since  $\sigma(A_0)$  is a closed set and  $\rho(A_0)$  is an open set, the closure of the open region (5.8) yields (5.7).

$\sigma_p(A_0)$ : By lemma 4, it is equivalent to consider  $\sigma_p(D_0)$ , where  $D_0 : H^1(\mathbb{R}) \subset L^2(\mathbb{R}) \rightarrow L^2(\mathbb{R})$  is given by (5.5). Let  $h \in H^1(\mathbb{R})$  be a solution of  $D_0 h = \lambda h$  for some  $\lambda \in \mathbb{C}$ . Then,  $h = h(z)$  satisfies

$$h'(z) + \frac{\pi}{4} \tanh\left(\frac{\pi z}{4}\right) h(z) + \frac{\pi}{4} w(z) \langle w', h \rangle = \lambda h(z), \quad z \in \mathbb{R}, \quad (5.10)$$

subject to the orthogonality condition  $\lambda \langle w, h \rangle = 0$ . Substitution  $h(z) = \tilde{h}(z)w(z)$  reduces (5.10) to the form

$$\tilde{h}'(z) + \frac{\pi}{4} \langle ww', \tilde{h} \rangle = \lambda \tilde{h}(z), \quad z \in \mathbb{R}, \quad (5.11)$$

subject to the orthogonality condition  $\lambda \langle w^2, \tilde{h} \rangle = 0$ .

For  $\lambda = 0$ , the general solution of equation (5.11) is  $\tilde{h}(z) = c_1 + c_2 z$ , where  $(c_1, c_2)$  are arbitrary constants. This yields the general solution  $h(z) = (c_1 + c_2 z)w(z)$  of equation (5.10) for  $\lambda = 0$ . Since  $h \in H^1(\mathbb{R})$ , then  $0 \in \sigma_p(D_0)$ .

For  $\lambda \neq 0$ , the general solution of equation (5.11) is a scalar multiplier of the particular solution

$$\tilde{h}(z) = e^{\lambda z} + \frac{\pi}{4\lambda} \langle ww', e^{\lambda z} \rangle, \quad (5.12)$$

where the inner product is defined for  $|\operatorname{Re}(\lambda)| < \frac{\pi}{2}$ . Since

$$\frac{\pi}{8} \|w\|^2 = \frac{1}{2} \int_{\mathbb{R}} \operatorname{sech}^2(z) dz = 1,$$

the orthogonality condition  $\lambda \langle w^2, \tilde{h} \rangle = 0$  is satisfied for the solution (5.12). Integration by parts and transformation back to  $h$  yields the solution

$$h(z) = e^{\lambda z} w(z) - \frac{\pi}{8} w(z) \langle w^2, e^{\lambda z} \rangle,$$

which show that  $h \in H^1(\mathbb{R})$  if and only if  $|\operatorname{Re}(\lambda)| < \frac{\pi}{4}$ , so that  $\sigma_p(A_0) = \sigma_p(D_0)$  is given by (5.8).

$\rho(A_0)$ : By lemma 4, it is equivalent to consider  $\rho(D_0)$ . Let  $h \in H^1(\mathbb{R})$  be a solution of  $(D_0 - \lambda)h = f$  for some  $\lambda \in \mathbb{C}$  and  $f \in L^2(\mathbb{R})$ . Then,  $h = h(z)$  satisfies

$$h'(z) + \frac{\pi}{4} \tanh\left(\frac{\pi z}{4}\right) h(z) + \frac{\pi}{4} w(z) \langle w', h \rangle = \lambda h(z) + f(z), \quad z \in \mathbb{R}. \quad (5.13)$$

Since  $\langle w, D_0 h \rangle = 0$ , we have  $\lambda \langle w, h \rangle + \langle w, f \rangle = 0$ . Multiplying equation (5.13) by  $\bar{h}$ , integrating over  $\mathbb{R}$ , adding complex conjugation and dividing by 2 yields

$$\frac{\pi}{4} \langle \tanh\left(\frac{\pi z}{4}\right) h, h \rangle + \frac{\pi}{4} \operatorname{Re} \langle h, w \rangle \langle w', h \rangle = \operatorname{Re}(\lambda) \|h\|^2 + \operatorname{Re} \langle h, f \rangle.$$

By Cauchy–Schwarz inequality and the constraint  $\bar{\lambda} \langle h, w \rangle + \langle f, w \rangle = 0$ , we obtain

$$\begin{aligned} \left( \operatorname{Re}(\lambda) - \frac{\pi}{4} \right) \|h\|^2 &\leq \operatorname{Re}(\lambda) \|h\|^2 - \frac{\pi}{4} \langle \tanh\left(\frac{\pi z}{4}\right) h, h \rangle \\ &= -\operatorname{Re} \langle h, f \rangle - \operatorname{Re} \frac{\pi}{4\lambda} \langle f, w \rangle \langle w', h \rangle \\ &\leq \left( 1 + \frac{\pi \|w\| \|w'\|}{4|\lambda|} \right) \|h\| \|f\| \end{aligned}$$

and

$$\begin{aligned} \left( -\operatorname{Re}(\lambda) - \frac{\pi}{4} \right) \|h\|^2 &\leq -\operatorname{Re}(\lambda) \|h\|^2 + \frac{\pi}{4} \langle \tanh\left(\frac{\pi z}{4}\right) h, h \rangle \\ &= \operatorname{Re} \langle h, f \rangle + \operatorname{Re} \frac{\pi}{4\lambda} \langle f, w \rangle \langle w', h \rangle \\ &\leq \left( 1 + \frac{\pi \|w\| \|w'\|}{4|\lambda|} \right) \|h\| \|f\|. \end{aligned}$$

This yields the bound

$$\|h\| \leq (1 + \|w\| \|w'\|) \frac{\|f\|}{|\operatorname{Re}(\lambda) - \frac{\pi}{4}|}, \quad \text{for } |\operatorname{Re}(\lambda)| > \frac{\pi}{4}.$$

Hence,  $\{\lambda \in \mathbb{C} : |\operatorname{Re}(\lambda)| > \frac{\pi}{4}\}$  belongs to  $\rho(D_0)$ , but since  $\sigma(D_0)$  is a closed set and  $\rho(D_0)$  is an open set, then  $\{\lambda \in \mathbb{C} : |\operatorname{Re}(\lambda)| > \frac{\pi}{4}\}$  is equivalent to  $\rho(D_0)$  in view of the location of  $\sigma_p(D_0)$ . This completes the proof of  $\rho(A_0) = \rho(D_0)$  given by (5.9).  $\square$

## 6. Full linearised evolution

The full linearised evolution is defined by the linear operator  $A : \mathcal{D} \subset L^2(\mathbb{T}) \rightarrow L^2(\mathbb{T})$  given by (4.14). The following theorem prescribes the spectrum of  $A$ .

**Theorem 3.** *The spectrum of  $A : \mathcal{D} \subset L^2(\mathbb{T}) \rightarrow L^2(\mathbb{T})$  completely covers the closed vertical strip given by*

$$\sigma(A) = \left\{ \lambda \in \mathbb{C} : -\frac{\pi}{4} \leq \operatorname{Re}(\lambda) \leq \frac{\pi}{4} \right\}. \quad (6.1)$$

*Proof.* Again, we obtain  $\sigma_p(A)$  and  $\rho(A)$  as

$$\sigma_p(A) = \left\{ \lambda \in \mathbb{C} : -\frac{\pi}{4} < \operatorname{Re}(\lambda) < \frac{\pi}{4} \right\} = \sigma_p(A_0), \quad (6.2)$$

$$\rho(A) = \left\{ \lambda \in \mathbb{C} : |\operatorname{Re}(\lambda)| > \frac{\pi}{4} \right\} = \rho(A_0). \quad (6.3)$$

Since  $\sigma(A)$  is a closed set and  $\rho(A)$  is an open set, the closure of the open region (6.2) yields (6.1).

$\sigma_p(A)$ : Let  $f \in \mathcal{D}$  be a solution of  $Af = \lambda f$  for some  $\lambda \in \mathbb{C}$ . Then,  $f = f(x)$  satisfies

$$\frac{1}{4}x(2\pi - x)f'(x) + \frac{1}{4\pi} \int_0^{2\pi} (\pi - x)f(x)dx + \frac{1}{2}\Pi_0\partial_x^{-1}\Pi_0f = \lambda f(x), \quad 0 < x < 2\pi. \quad (6.4)$$

subject to the orthogonality condition  $\lambda \int_0^{2\pi} f(x)dx = 0$ .

If  $f \in \mathcal{D}$ , then  $f \in L^2(\mathbb{T})$  and  $(c_*^2 - 2\eta_*)f' \in L^2(\mathbb{T})$ , whereas  $\lim_{x \rightarrow 0^+} f(x)$  and  $\lim_{x \rightarrow 2\pi^-} f(x)$  may not be defined. Nevertheless, since  $c_*^2 - 2\eta_*(x) \neq 0$  for  $x \in (0, 2\pi)$ , we have  $f \in C^0(0, 2\pi)$ . Bootstrapping arguments for equation (6.4) imply that  $f \in C^\infty(0, 2\pi)$ . Differentiating (6.4) in  $x$  yields the second-order differential equation

$$\frac{1}{4}x(2\pi - x)f''(x) + \frac{1}{2}(\pi - x)f'(x) + \frac{1}{2}f(x) - \frac{1}{4\pi} \int_0^{2\pi} f(x)dx = \lambda f'(x), \quad 0 < x < 2\pi. \quad (6.5)$$

If  $\lambda \neq 0$ , then  $\int_0^{2\pi} f(x)dx = 0$  so that equation (6.5) can be rewritten in the form

$$\frac{1}{4}x(2\pi - x)f''(x) + \frac{1}{2}(\pi - x)f'(x) + \frac{1}{2}f(x) = \lambda f'(x), \quad 0 < x < 2\pi. \quad (6.6)$$

One solution of (6.6) is obtained explicitly as  $f_1(x) = 2\lambda - \pi + x$ . The second linearly independent solution  $f_2(x)$  of (6.6) is obtained from the Wronskian

$$f_1(x)f_2'(x) - f_1'(x)f_2(x) = W(x), \quad (6.7)$$

where  $W(x)$  satisfies the first-order differential equation by Abel's theorem:

$$W'(x) = \frac{2(2\lambda - \pi + x)}{x(2\pi - x)}W(x). \quad (6.8)$$

Integrating (6.8) yields

$$W(x) = \frac{\pi^2}{x(2\pi - x)} \left( \frac{x}{2\pi - x} \right)^{\frac{2\lambda}{\pi}}, \quad (6.9)$$

where the constant of integration has been normalised by the condition  $W(\pi) = 1$ . It follows from (6.7) and (6.9) that if  $\lambda \neq 0$ , then  $f_2(x)$  satisfies the following asymptotic limits

$$f_2(x) \sim \begin{cases} x^{\frac{2\lambda}{\pi}}, & \lambda \neq \frac{\pi}{2}, \\ 1, & \lambda = \frac{\pi}{2} \end{cases} \quad \text{as } x \rightarrow 0^+$$

and

$$f_2(x) \sim \begin{cases} (2\pi - x)^{-\frac{2\lambda}{\pi}}, & \lambda \neq -\frac{\pi}{2}, \\ 1, & \lambda = -\frac{\pi}{2} \end{cases} \quad \text{as } x \rightarrow (2\pi)^-.$$

On the other hand,  $f_1, f_2 \in C^\infty(0, 2\pi)$  for every  $\lambda \in \mathbb{C}$ .

If  $|\operatorname{Re}(\lambda)| < \frac{\pi}{4}$ , then  $f_2 \in L^2(\mathbb{T})$  and  $(c_*^2 - \eta_*)f_2' \in L^2(\mathbb{T})$ , so that  $f(x) = c_1 f_1(x) + c_2 f_2(x)$  belongs to  $\mathcal{D}$  for every  $(c_1, c_2) \in \mathbb{R}^2$ . Satisfying the constraint  $\int_0^{2\pi} f(x) dx = 0$  for  $\lambda \neq 0$  yields a one-parameter family of solutions  $f \in \mathcal{D}$  of (6.4) for every  $\lambda \in \sigma_p(A) \setminus \{0\}$ , where  $\sigma_p(A)$  is given by (6.2).

If  $\lambda = 0$ , then equation (6.5) contains a constant term. Without the constant term  $-\frac{1}{4\pi} \int_0^{2\pi} f(x) dx$ , the two homogeneous solutions  $f_1, f_2 \in \mathcal{D}$  are given by

$$f_1(x) = x - \pi, \quad f_2(x) = \frac{1}{2\pi}(x - \pi) \ln \frac{x}{2\pi - x} - 1,$$

However, only  $f_1$  satisfies (6.5) since  $\int_0^{2\pi} f_1(x) dx = 0$ . On the other hand, it is easy to see that  $f(x) = 1$  is also a solution of (6.5). Thus, there exists a two-parameter family of solutions  $f = c_1(x - \pi) + c_2 \in \mathcal{D}$  of equation (6.4) for  $\lambda = 0$ , so that  $0 \in \sigma_p(A)$ .

Finally, if  $|\operatorname{Re}(\lambda)| \geq \frac{\pi}{4}$ , then  $f_2 \notin L^2(\mathbb{T})$  due to the asymptotic limits as  $x \rightarrow 0^+$  and  $x \rightarrow (2\pi)^-$ . On the other hand,  $\int_0^{2\pi} f_1(x) dx = 4\pi\lambda \neq 0$  for  $\lambda \neq 0$ , so that there exist no nonzero solutions  $f \in \mathcal{D}$  of equation (6.4) for every  $\lambda \notin \sigma_p(A)$ . This completes the proof of  $\sigma_p(A)$  given by (6.2).

$\rho(A)$ : Let  $f \in \mathcal{D}$  be a solution of the resolvent equation  $(A - \lambda)f = g$  for  $g \in L^2(\mathbb{T})$  rewritten in the form:

$$(c_*^2 - 2\eta_*)\partial_x f - \frac{1}{\pi} \oint \eta'_* f dx + \frac{1}{2} \Pi_0 \partial_x^{-1} \Pi_0 f - \lambda f = g, \quad x \in \mathbb{T}. \quad (6.10)$$

Since  $\oint A f dx = 0$ , we get  $-\lambda \oint f dx = \oint g dx$ . Taking into account that  $\Pi_0 \partial_x^{-1} \Pi_0$  is a skew-adjoint operator in  $L^2(\mathbb{T})$ , we multiply (6.10) by  $\bar{f}$ , integrate over  $\mathbb{T}$ , add a complex conjugate equation and divide by 2 to obtain

$$\operatorname{Re}\langle f, (c_*^2 - 2\eta_*)\partial_x f \rangle - \operatorname{Re}(\lambda)\|f\|^2 - \frac{1}{\pi} \operatorname{Re}\langle f, 1 \rangle \langle \eta'_*, f \rangle = \operatorname{Re}\langle f, g \rangle.$$

Integrating by parts in the first term and using  $-\bar{\lambda}\langle f, 1 \rangle = \langle g, 1 \rangle$  for  $\lambda \neq 0$ , we obtain

$$\langle \eta'_* f, f \rangle - \operatorname{Re}(\lambda)\|f\|^2 + \operatorname{Re} \frac{\langle \eta'_*, f \rangle \langle g, 1 \rangle}{\pi \bar{\lambda}} = \operatorname{Re}\langle f, g \rangle.$$

Since  $-\frac{\pi}{4} \leq \eta'_*(x) \leq \frac{\pi}{4}$  for  $x \in [0, 2\pi]$ , we get by Cauchy–Schwarz inequality that

$$\begin{aligned} \left( \operatorname{Re}(\lambda) - \frac{\pi}{4} \right) \|f\|^2 &\leq \operatorname{Re}(\lambda)\|f\|^2 - \langle \eta'_* f, f \rangle \\ &= -\operatorname{Re}\langle f, g \rangle + \operatorname{Re} \frac{\langle \eta'_*, f \rangle \langle g, 1 \rangle}{\pi \bar{\lambda}} \\ &\leq \left( 1 + \frac{\sqrt{2\pi} \|\eta'_*\|}{\pi |\lambda|} \right) \|g\| \|f\| \end{aligned}$$

and

$$\begin{aligned} \left( -\operatorname{Re}(\lambda) - \frac{\pi}{4} \right) \|f\|^2 &\leq -\operatorname{Re}(\lambda)\|f\|^2 + \langle \eta'_* f, f \rangle \\ &= \operatorname{Re}\langle f, g \rangle - \operatorname{Re} \frac{\langle \eta'_*, f \rangle \langle g, 1 \rangle}{\pi \bar{\lambda}} \\ &\leq \left( 1 + \frac{\sqrt{2\pi} \|\eta'_*\|}{\pi |\lambda|} \right) \|g\| \|f\|. \end{aligned}$$

This yields the bound

$$\|f\| \leq \left(1 + \frac{4\sqrt{2\pi}\|\eta'_*\|}{\pi^2}\right) \frac{\|g\|}{|\operatorname{Re}(\lambda)| - \frac{\pi}{4}}, \quad \text{for } |\operatorname{Re}(\lambda)| > \frac{\pi}{4}.$$

Hence,  $\{\lambda \in \mathbb{C} : |\operatorname{Re}(\lambda)| > \frac{\pi}{4}\}$  belongs to  $\rho(A)$ , but since  $\sigma(A)$  is a closed set and  $\rho(A)$  is an open set, then  $\{\lambda \in \mathbb{C} : |\operatorname{Re}(\lambda)| > \frac{\pi}{4}\}$  is equivalent to  $\rho(A)$  in view of the location of  $\sigma_p(A)$  in (6.2). This completes the proof of  $\rho(A)$  given by (6.3).  $\square$

**Remark 6.** Since the intersections of  $\sigma_p(A) \cap \rho(A_0)$  and  $\sigma_p(A_0) \cap \rho(A)$  are empty, as follows from (5.8), (5.9), (6.2) and (6.3), the result  $\sigma(A) = \sigma(A_0)$  also follows by theorem 1 in [22]. Computations in the proof of theorem 3 do not rely on the truncated operator  $A_0 : \mathcal{D} \subset L^2(\mathbb{T}) \rightarrow L^2(\mathbb{T})$  introduced and studied in section 5. We included these computations anyway to emphasise that the linear instability of the peaked travelling wave is induced by the quasilinear part of the inviscid Burgers equation and that the dispersion term of the evolution equation (2.2) does not play the role. This has been the main property of the linear instability of the peaked travelling wave in the Camassa–Holm equation [30, 39, 41], the reduced Ostrovsky equation [21, 22] and the Novikov equation [10, 29].

## 7. Nonlinear evolution

We shall now derive the nonlinear instability result for the peaked travelling wave by using the nonlinear evolution equation (4.4). With the help of equations (4.9) and (4.11) in lemma 2, we rewrite the nonlinear evolution equation (4.4) in the equivalent form:

$$2c_*\partial_t\zeta = (c_*^2 - 2\eta_*)\partial_x\zeta - 2(\zeta - \zeta|_{x=0})\partial_x\zeta - \frac{1}{\pi} \oint \eta'_*\zeta dx + \frac{1}{2}\Pi_0\partial_x^{-1}\Pi_0 [\zeta + 2(\partial_x\zeta)^2]. \quad (7.1)$$

After applying the transformation (4.3) and integrating by parts using (3.5), the original constraint (2.1) becomes

$$0 = \oint [\zeta + 2\eta'_*\partial_x\zeta + (\partial_x\zeta)^2] dx = \frac{1}{2} \oint [\zeta + 2(\partial_x\zeta)^2] dx + \pi\zeta|_{x=0}. \quad (7.2)$$

The following lemma identifies two conserved quantities of the evolution equation (7.1), whose sum yields the constraint (7.2).

**Lemma 5.** Consider a local solution  $\zeta \in C^0((-\tau_0, \tau_0), H_{\text{per}}^1(\mathbb{T}) \cap W^{1,\infty}(\mathbb{T}))$  of the evolution equation (7.1) for some  $\tau_0 > 0$ . Then

$$\oint \zeta dx \quad \text{and} \quad \zeta|_{x=0} + \frac{1}{\pi} \oint (\partial_x\zeta)^2 dx \quad (7.3)$$

are conserved for  $t \in (-\tau_0, \tau_0)$ .

*Proof.* The conservation of  $\oint \zeta dx$  is shown by taking the mean value of the evolution equation (7.1), while the conservation of  $\zeta|_{x=0} + \frac{1}{\pi} \oint (\partial_x\zeta)^2 dx$  follows from the constraint (7.2). We can also show the



latter conservation directly as follows. For smooth solutions, we differentiate [equation \(7.1\)](#) and obtain

$$2c_*\partial_t\partial_x\zeta = (c_*^2 - 2\eta_*)\partial_x^2\zeta - 2\eta'_*\partial_x\zeta - 2(\zeta - \zeta|_{x=0})\partial_x^2\zeta - 2(\partial_x\zeta)^2 + \frac{1}{2}(\zeta + 2(\partial_x\zeta)^2) - \frac{1}{4\pi}\oint(\zeta + 2(\partial_x\zeta)^2)dx \quad (7.4)$$

Multiplying [\(7.4\)](#) by  $\partial_x\zeta$  and integrating in  $x$  over  $\mathbb{T}$  yields

$$c_*\frac{d}{dt}\oint(\partial_x\zeta)^2dx = -\oint\eta'_*(\partial_x\zeta)^2dx. \quad (7.5)$$

Furthermore, taking the limit  $x \rightarrow 0$  in [equation \(7.1\)](#) as in [\(4.12\)](#) and [\(4.13\)](#), we get

$$2c_*\lim_{x \rightarrow 0}\partial_t\zeta = \lim_{x \rightarrow 0}\Pi_0\partial_x^{-1}\Pi_0(\partial_x\zeta)^2 = \frac{2}{\pi}\oint\eta'_*(\partial_x\zeta)^2dx. \quad (7.6)$$

By adding [\(7.5\)](#) divided by  $\pi$  and [\(7.6\)](#) divided by 2, we verify conservation of  $\zeta|_{x=0} + \frac{1}{\pi}\oint(\partial_x\zeta)^2dx$ . By Sobolev's embedding of  $H_{\text{per}}^1(\mathbb{T})$  into  $C_{\text{per}}^0(\mathbb{T})$ , we have well-defined  $\zeta|_{x=0} \in C^0(-\tau_0, \tau_0)$ . Hence, the conserved quantities [\(7.3\)](#) are well-defined for the local solution  $\zeta \in C^0((-\tau_0, \tau_0), H_{\text{per}}^1(\mathbb{T}) \cap W^{1,\infty}(\mathbb{T}))$ .  $\square$

Based on the conserved quantity  $\zeta|_{x=0} + \frac{1}{\pi}\oint(\partial_x\zeta)^2dx$ , we obtain the nonlinear instability of the peaked travelling wave given by the following theorem.

**Theorem 4.** *For every  $\delta > 0$  there exists  $\zeta_0 \in H_{\text{per}}^1(\mathbb{T}) \cap W^{1,\infty}(\mathbb{T})$  satisfying*

$$\|\zeta_0\|_{H_{\text{per}}^1} \leq \delta^2, \quad \|\zeta_0\|_{W^{1,\infty}} \leq \delta, \quad (7.7)$$

*such that the unique local solution  $\zeta \in C^0((-\tau_0, \tau_0), H_{\text{per}}^1(\mathbb{T}) \cap W^{1,\infty}(\mathbb{T}))$  of the evolution [equation \(7.1\)](#) with  $\zeta|_{t=0} = \zeta_0$  satisfies*

$$\|\zeta(t_0, \cdot)\|_{W^{1,\infty}} = 1, \quad (7.8)$$

*for some  $t_0 \in (0, \tau_0)$ .*

*Proof.* The proof follows by the method of characteristics which works for every local solution  $\zeta \in C^0((-\tau_0, \tau_0), H_{\text{per}}^1(\mathbb{T}) \cap W^{1,\infty}(\mathbb{T}))$  of the evolution [equation \(7.1\)](#). Let  $x = X(t, s)$  be the family of characteristic curves for  $(t, s) \in (-\tau_0, \tau_0) \times (0, 2\pi)$  obtained from

$$\begin{cases} 2c_*\partial_t X(t, s) = -(c_*^2 - 2\eta_*(X)) + 2(\zeta(t, X) - \zeta(t, 0)), \\ X(0, s) = s. \end{cases} \quad (7.9)$$

Since the vector field of the initial-value problem [\(7.9\)](#) is Lipschitz for the local solution  $\zeta \in C^0((-\tau_0, \tau_0), H_{\text{per}}^1(\mathbb{T}) \cap W^{1,\infty}(\mathbb{T}))$ , there is a unique solution for  $X \in C^1((-\tau_0, \tau_0) \times (0, 2\pi))$  such that  $X(t, 0) = 0$  and  $X(t, 2\pi) = 2\pi$ . Since  $[0, 2\pi]$  is the fundamental period of  $\mathbb{T}$ , we also get  $\zeta(t, 0) = \zeta(t, 2\pi)$ . By solving the linear equation for  $\partial_s X(t, s)$ , we get

$$\partial_s X(t, s) = \exp\left(\frac{1}{c_*}\int_0^t [\eta'_*(X(t', s)) + \partial_x\zeta(t', X(t', s))] dt'\right),$$

from which it follows that  $\partial_s X(t, s) > 0$  for every  $t \in (-\tau_0, \tau_0)$  and  $s \in (0, 2\pi)$ . Hence the mapping  $[0, 2\pi] \ni s \mapsto X(t, s) \in [0, 2\pi]$  is a diffeomorphism for  $t \in (-\tau_0, \tau_0)$ .

To proceed further, we consider the restriction of  $\zeta_0 \in H_{\text{per}}^1(\mathbb{T}) \cap W^{1,\infty}(\mathbb{T}) \cap C^1(0, 2\pi)$ . Along the family of characteristic curves, we can now define  $Z(t, s) := \zeta(t, X(t, s))$  and  $V(t, s) := \partial_x \zeta(t, X(t, s))$ . By using the evolution equations (7.1) and (7.4) along the family of characteristic curves satisfying (7.9), we obtain the following initial-value problems:

$$\begin{cases} 2c_* \partial_t Z(t, s) = -\frac{1}{\pi} \langle \eta'_*, \zeta \rangle + \frac{1}{2} \Pi_0 \partial_x^{-1} \Pi_0 (\zeta + 2(\partial_x \zeta)^2), \\ Z(0, s) = \zeta_0(s), \end{cases} \quad (7.10)$$

and

$$\begin{cases} 2c_* \partial_t V(t, s) = -2\eta'_*(X) V - V^2 + \frac{1}{2} (Z(t, s) + Z(t, 0)), \\ V(0, s) = \zeta'_0(s), \end{cases} \quad (7.11)$$

where we have used the constraint (7.2). If  $\zeta_0 \in H_{\text{per}}^1(\mathbb{T}) \cap W^{1,\infty}(\mathbb{T}) \cap C^1(0, 2\pi)$ , then the solutions of the initial-value problems (7.9), (7.10) and (7.11) are defined in the class of functions

$$\begin{cases} X \in C^1((-\tau_0, \tau_0) \times (0, 2\pi)), \\ Z \in C^1((-\tau_0, \tau_0) \times (0, 2\pi)), \\ V \in C^1((-\tau_0, \tau_0), C^0(0, 2\pi)), \end{cases}$$

respectively, with the bounded one-sided limits as  $s \rightarrow 0^+$  and  $s \rightarrow (2\pi)^-$ . Due to the conservation law in (7.3), we have

$$\zeta|_{x=0} + \frac{1}{\pi} \oint (\partial_x \zeta)^2 dx = C_0,$$

from which  $\zeta|_{x=0} \leq C_0$  with a time-independent positive constant  $C_0$ . Since  $X(t, 0) = 0$ , we get  $Z(t, 0) \leq C_0$  so that the evolution problem (7.11) in the limit  $s \rightarrow 0^+$  yields for  $V_0(t) := \lim_{s \rightarrow 0^+} V(t, s)$ :

$$2c_* V'_0(t) = \frac{\pi}{2} V_0(t) - V_0^2(t) + Z(t, 0) \leq \frac{\pi}{2} V_0(t) + C_0.$$

Iterating the inequality as

$$2c_* \frac{d}{dt} e^{-\frac{\pi t}{4c_*}} V_0(t) \leq C_0 e^{-\frac{\pi t}{4c_*}}$$

and integrating yields

$$2c_* \left[ e^{-\frac{\pi t}{4c_*}} V_0(t) - V_0(0) \right] \leq \frac{4c_* C_0}{\pi} \left[ 1 - e^{-\frac{\pi t}{4c_*}} \right] \leq \frac{4c_* C_0}{\pi}.$$

This implies

$$V_0(t) \leq \left( V_0(0) + \frac{2}{\pi} C_0 \right) e^{\frac{\pi t}{4c_*}}.$$

If the initial bound (7.7) is true, we get by Sobolev embedding of  $H_{\text{per}}^1(\mathbb{T})$  to  $L^\infty(\mathbb{T})$  that

$$|C_0| \leq \delta^2 + \frac{1}{\pi} \delta^2 \leq 2\delta^2,$$

so that the interval  $(-\delta, -\frac{2}{\pi}|C_0|)$  is nonempty for all sufficiently small  $\delta > 0$ . Selecting  $-\delta < V_0(0) < -\frac{2}{\pi}|C_0|$  to satisfy the initial bound (7.7) and to ensure that  $V_0(0) + \frac{2}{\pi}C_0 < 0$  yields the exponential divergence  $V_0(t) \rightarrow -\infty$  as  $t \rightarrow +\infty$ . Since  $\tau_0 > 0$  is the maximal existence time in  $H_{\text{per}}^1(\mathbb{T}) \cap W^{1,\infty}(\mathbb{T})$  norm, there exists  $t_0 \in (0, \tau_0)$  such that the instability bound (7.8) holds.  $\square$

**Remark 7.** By incorporating the quadratic term in the bound

$$2c_* V_0'(t) = \frac{\pi}{2} V_0(t) - V_0^2(t) + Z(t, 0) \leq \frac{\pi}{2} V_0(t) - V_0^2(t) + C_0,$$

one can find initial data  $\zeta_0 \in H_{\text{per}}^1(\mathbb{T}) \cap W^{1,\infty}(\mathbb{T})$  for which  $\|\zeta(t, \cdot)\|_{W^{1,\infty}}$  diverges in a finite time, see [39] for a similar analysis of the Camassa–Holm equation. However, we do not have the bound on  $\|\zeta(t, \cdot)\|_{H_{\text{per}}^1}$  compared to the case of the Camassa–Holm equation, where the  $H_{\text{per}}^1$  norm of the perturbation does not grow in time, see [32, 33, 39].

## 8. Numerical approximations

We approximate numerically the smooth profile  $\eta \in C_{\text{per}}^\infty(\mathbb{T})$  of the travelling waves from the second-order equation (3.1) and the eigenvalues of the Hessian operator  $\mathcal{L} : H_{\text{per}}^2(\mathbb{T}) \subset L^2(\mathbb{T}) \rightarrow L^2(\mathbb{T})$  which defines the linearised time evolution (4.1) for the smooth travelling waves. In both cases, we are interested to understand the convergence of numerical results to the peaked travelling wave with the profile  $\eta_* \in C_{\text{per}}^0(\mathbb{T}) \cap W^{1,\infty}(\mathbb{T})$  as  $c \rightarrow c_*$ . We show that the lowest eigenvalue of  $\mathcal{L}$  diverges as  $c \rightarrow c_*$ , which suggests that the linearised equation (4.1) cannot be used for the peaked travelling wave. This explains why we had to derive a different linearised equation (4.5) for the peaked travelling wave.

To obtain the solutions  $\eta \in C_{\text{per}}^\infty(\mathbb{T})$  of the second-order equation (3.1) for  $c \in (1, c_*)$ , we use the first-order invariant (3.2) and define  $\eta$  from the boundary-value problem:

$$\begin{cases} \left(\frac{d\eta}{dx}\right)^2 = \frac{2\mathcal{E} - \eta^2}{c^2 - 2\eta}, \\ \eta(\pm\pi) = -\sqrt{2\mathcal{E}}. \end{cases} \quad (8.1)$$

Since  $\eta(-x) = \eta(x)$ , we take the negative sign in the square root of (8.1) for  $x \in [0, \pi]$  and obtain the solution profile  $\eta(x)$  for  $x \in [0, \pi]$  by finding the root of the integral equation

$$f(\eta(x)) - x = 0, \quad f(\eta) := \int_{\eta/\sqrt{2\mathcal{E}}}^1 \frac{\sqrt{c^2 - 2\sqrt{2\mathcal{E}}x}}{\sqrt{1 - x^2}} dx, \quad (8.2)$$

for  $\mathcal{E} \in (0, \mathcal{E}_c)$ , where  $\mathcal{E}_c := \frac{c_*^4}{8}$  is the value separating smooth and cusped profiles.

To determine the value of  $\mathcal{E}$  for each  $c \in (1, c_*)$ , we consider the period function  $T(\mathcal{E}, c)$  studied in [36]. The period function is represented by using the complete elliptic integral  $E(\kappa)$  of the second kind with the elliptic modulus  $\kappa \in (0, 1)$ , which is defined by  $\mathcal{E} \in (0, \mathcal{E}_c)$  and  $c \in (1, c_*)$  as follows:

$$T(\mathcal{E}, c) = 4E(\kappa)\sqrt{c^2 + 2\sqrt{2\mathcal{E}}}, \quad \kappa = \sqrt{\frac{4\sqrt{2\mathcal{E}}}{c^2 + 2\sqrt{2\mathcal{E}}}}. \quad (8.3)$$

The periodic profile  $\eta \in C_{\text{per}}^\infty(\mathbb{T})$  corresponds to the value of  $\mathcal{E} = \mathcal{E}(c)$  found from the root of  $T(\mathcal{E}(c), c) = 2\pi$ .

To approximate the solution profile numerically, we let  $x_j = jh, j \in \{0, \dots, N\}$  be a fixed grid with the step size  $h = \pi/N$  for a large integer  $N$ . By the fundamental theorem of calculus, the solution profile

$\{(x_j, \eta_j)\}_{j=0}^N$  can be found by solving  $f(\eta_j) - x_j = 0$  for every  $j$ . We implement Newton–Raphson’s method as the root-finding algorithm under a specific tolerance  $\epsilon > 0$ , such that

$$\eta_j^{(k+1)} = \eta_j^{(k)} - \frac{1}{f'(\eta_j^{(k)})} \left[ f(\eta_j^{(k)}) - x_j \right], \quad \left| f(\eta_j^{(k)}) - x_j \right| < \epsilon, \quad (8.4)$$

where  $k \in \mathbb{N}$  denotes iteration number, and we take  $\eta_0^{(k)}(0) = \sqrt{2\mathcal{E}}$  and  $\eta_N^{(k)}(\pi) = -\sqrt{2\mathcal{E}}$  as two boundary grid points for any  $k$  to avoid the singularities. Given a  $c$ -grid  $\{c_i\}_{i=1}^M$  with  $M$  grid points, we compute  $\mathcal{E}_i := \mathcal{E}(c_i)$  from the period function (8.3) by solving numerically  $T(\mathcal{E}_i, c_i) = 2\pi$ . This outputs the sets of parameter pairs  $\{(c_i, \mathcal{E}_i)\}_{i=1}^M$ , which can be used in the root-finding algorithm (8.4). After the solution  $\{(x_j, \eta_j)\}_{j=0}^N$  is obtained on  $[0, \pi]$  for  $N+1$  grid points, the even reflection fills all  $2N+1$  grid points on  $[-\pi, \pi]$  domain. The solution points  $\{(x_j, \eta_j)\}_{j=-N}^N$  are plotted in figure 1 (left) and the parameter pairs  $\{(c_i, \sqrt{2\mathcal{E}_i})\}_{i=1}^M$  are plotted in figure 1 (right).

The solution  $\{(x_j, \eta_j)\}_{j=-N}^N$  can be represented in Fourier space by using the discrete Fourier transform (DFT) with  $2N+1$  modes:

$$\hat{\eta}_n = \frac{h}{2\pi} \sum_{j=-N}^{N-1} \eta_j e^{-inx_j}, \quad n \in \{-N, \dots, N\} \quad (8.5)$$

where one of the endpoints  $x_N = \pi$  in the physical space is removed due to the  $2\pi$ -periodicity. For the peaked wave profile  $\eta_*$  at  $c = c_*$ , the solution (3.3) can be represented as the Fourier cosine series

$$\eta_*(x) = -\frac{\pi^2}{48} + \sum_{m=1}^{\infty} \frac{\cos(mx)}{2m^2}. \quad (8.6)$$

By applying DFT on the selected grid, the solution points  $\{(n, \hat{\eta}_n)\}_{n=0}^N$  are plotted for the smooth profiles in figure 2. The black dashed line represents the Fourier series (8.6) for the peaked profile. We note that the fast convergence of the Fourier transform for the smooth waves is replaced by the slow convergence  $\mathcal{O}(m^{-2})$  of the Fourier transform for the peaked waves.

Next, we study numerically the spectrum of the Hessian operator  $\mathcal{L} : H_{\text{per}}^2(\mathbb{T}) \subset L^2(\mathbb{T}) \rightarrow L^2(\mathbb{T})$  which appears in the linearised equation (4.1). The spectrum of  $\mathcal{L}$  can be computed by solving the spectral problem with the  $2\pi$ -periodic conditions,

$$\mathcal{L}\gamma = \lambda\gamma, \quad \gamma \in H_{\text{per}}^2(\mathbb{T}). \quad (8.7)$$

We will apply two numerical methods (the finite-difference method and the Fourier collocation method) to solve the spectral problem (8.7). We write  $\mathcal{L} = \mathcal{M} + \mathcal{W}$  with  $\mathcal{M} = -\partial_x(c^2 - 2\eta)\partial_x$  and  $\mathcal{W} = (2\eta'' - 1)$ .

For the finite difference method, using the numerical approximation of the solution profile  $\{(x_j, \eta_j)\}_{j=-N}^N$  and the central difference approximation of the second derivative  $\mathcal{M}$ , we construct the differentiation matrix for  $\mathcal{L}$  acting on the eigenvector  $\gamma = (\gamma_{-N}, \dots, \gamma_{N-1}) \in \mathbb{R}^{2N}$ ,

$$\mathcal{L} = \begin{bmatrix} (W^0 + \mathcal{M}^0)(\eta_{-N}) & \mathcal{M}^{+1}(\eta_{-N}) & 0 & \cdots & \mathcal{M}^{-1}(\eta_N) \\ \mathcal{M}^{-1}(\eta_{-N+1}) & (\mathcal{W}^0 + \mathcal{M}^0)(\eta_{-N+1}) & \mathcal{M}^{+1}(\eta_{-N+1}) & \cdots & 0 \\ 0 & \mathcal{M}^{-1}(\eta_{-N+2}) & (W^0 + \mathcal{M}^0)(\eta_{-N+2}) & \cdots & 0 \\ \vdots & \vdots & \vdots & \ddots & \vdots \\ \mathcal{M}^{+1}(\eta_{N-1}) & 0 & 0 & \cdots & (\mathcal{W}^0 + \mathcal{M}^0)(\eta_{N-1}) \end{bmatrix},$$

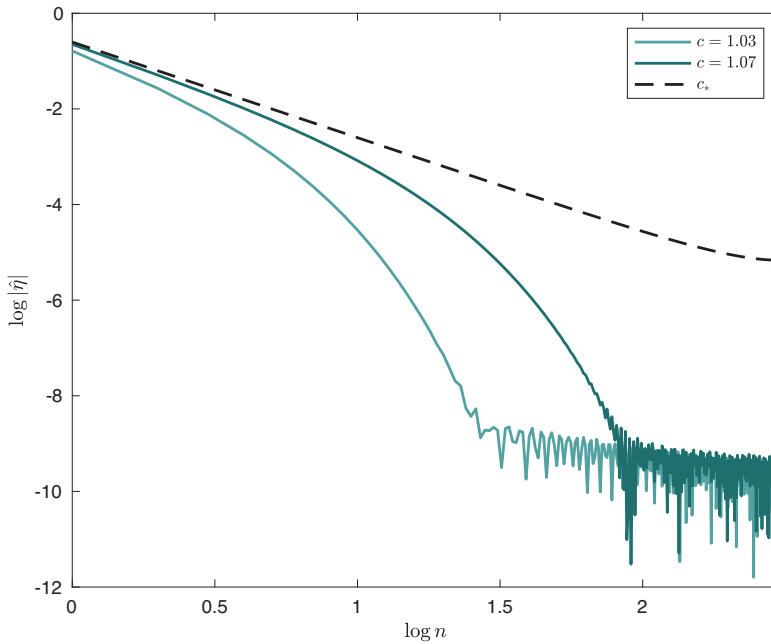


**Figure 2.** The solution profiles  $\hat{\eta}$  in Fourier space (8.5) in log-log coordinates for  $c = 1.03, 1.07$  with  $N = 300$  grid points and  $\epsilon = 10^{-14}$  tolerance. The black dashed line represents the peaked profile  $\eta_*$  for  $c = c_*$ .

where the boundary point  $x_N = \pi$  is removed due to the  $2\pi$ -periodicity. The diagonal elements  $\mathcal{M}^0(\eta_j)$ ,  $\mathcal{W}^0(\eta_j)$  and the off-diagonal elements  $\mathcal{M}^{\pm 1}(\eta_j)$  for  $j \in \{-N, \dots, N-1\}$  can be written as

$$\mathcal{M}^0(\eta_j) = \frac{2c^2 - 2\eta_j - \eta_{j+1} - \eta_{j-1}}{h^2}, \quad \mathcal{M}^{\pm 1}(\eta_j) = -\frac{c^2 - \eta_j - \eta_{j\pm 1}}{h^2},$$

and

$$\mathcal{W}^0(\eta_j) = \frac{4\mathcal{E} + 2\eta_j^2 - 2c^2\eta_j}{(c^2 - 2\eta_j)^2} - 1$$

for  $c \in (1, c_*)$ , where the differential equations (3.1) and (3.2) have been used to eliminate  $\eta''(x)$ . By numerically solving the eigenvalue problem, we obtain the first four eigenfunctions  $\gamma$  plotted in figure 3. The eigenfunctions display spikes near  $x = 0$  in the limit of  $c \rightarrow c_*$ .

For the Fourier collocation method, we use the discrete Fourier transform (8.5) and represent  $\gamma$  in the spectral problem (8.7) by  $\hat{\gamma} = (\hat{\gamma}_{-N}, \dots, \hat{\gamma}_N) \in \mathbb{R}^{2N+1}$ . Thanks to the  $L^2$ -isomorphism between functions in physical and Fourier spaces, the eigenvalue problem in Fourier space  $\hat{\mathcal{L}}\hat{\gamma} = \lambda\hat{\gamma}$  shares the same eigenvalues as that in the physical space. We write again  $\hat{\mathcal{L}} = \hat{\mathcal{M}} + \hat{\mathcal{W}}$  with

$$\hat{\mathcal{M}} = 2(\mathcal{D}_1\hat{\eta})\mathcal{D}_1 - c^2\mathcal{D}_2 + 2\hat{\eta}\mathcal{D}_2, \quad \hat{\mathcal{W}} = 2(\mathcal{D}_2\hat{\eta}) - \pi I$$

for  $c \in (1, c_*)$ , where the first and second derivative are represented by

$$\mathcal{D}_1 = i \operatorname{diag}(-N, \dots, N), \quad \mathcal{D}_2 = \mathcal{D}_1^2$$

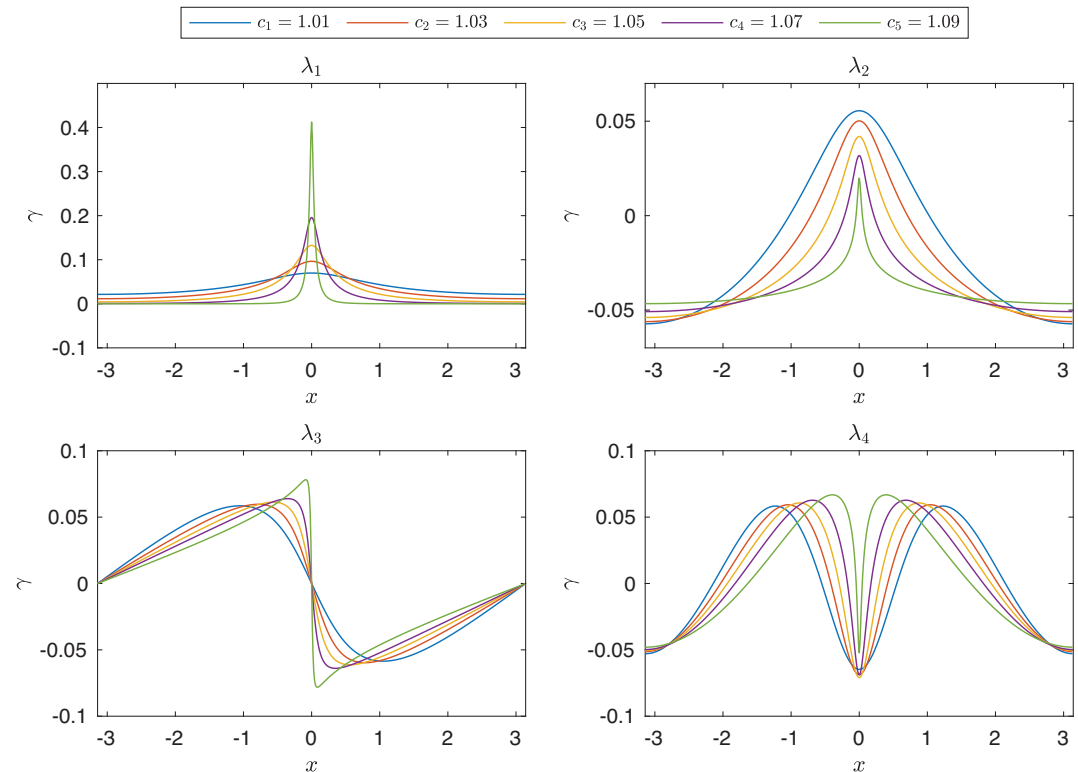


**Figure 3.** Eigenfunctions corresponding to the first four eigenvalues for five values of  $c$  in  $(1, c_*)$ . The grid in physical space is chosen to be  $N = 300$ . The solution profiles obtained from equation (8.4) are used, and all eigenfunctions are plotted on  $[-\pi, \pi]$  with positive slope near  $-\pi$ .

and  $\hat{\eta}$  is the Toeplitz matrix for convolution with the Fourier modes for  $m \in \{-N, \dots, N\}$ ,

$$\hat{\eta} = \begin{bmatrix} \hat{\eta}_0 & \cdots & \hat{\eta}_{-N} & \cdots & 0 \\ \vdots & \ddots & \vdots & \ddots & \vdots \\ \hat{\eta}_N & \cdots & \hat{\eta}_0 & \cdots & \hat{\eta}_{-N} \\ \vdots & \ddots & \vdots & \ddots & \vdots \\ 0 & \cdots & \hat{\eta}_N & \cdots & \hat{\eta}_0 \end{bmatrix}.$$

By numerically solving the eigenvalue problem in the Fourier space, we obtain the first four eigenfunctions plotted in figure 4. Convergence of eigenfunctions in Fourier space for large  $m$  becomes worse as  $c \rightarrow c_*$ .

Figure 5 shows the first four eigenvalues obtained by the finite-difference method (left) and the Fourier collocation method (right). The lowest eigenvalue diverges to  $-\infty$  as  $c \rightarrow c_*$ . After  $\lambda_1$ , the even-numbered eigenvalues  $\lambda_2, \lambda_4, \dots$  correspond to eigenfunctions of even parity in  $x$ , whereas the odd-numbered eigenvalues  $\lambda_3, \lambda_5, \dots$  correspond to eigenfunctions of odd parity. Convergence of eigenvalues as  $c \rightarrow c_*$  is low in both physical and Fourier space for the fixed truncation number  $N$ . The grey shaded region highlights the loss of precision in the numerical approximations of eigenvalues with poor convergence to the eigenvalues of the limiting peaked wave for  $N = 300$ .

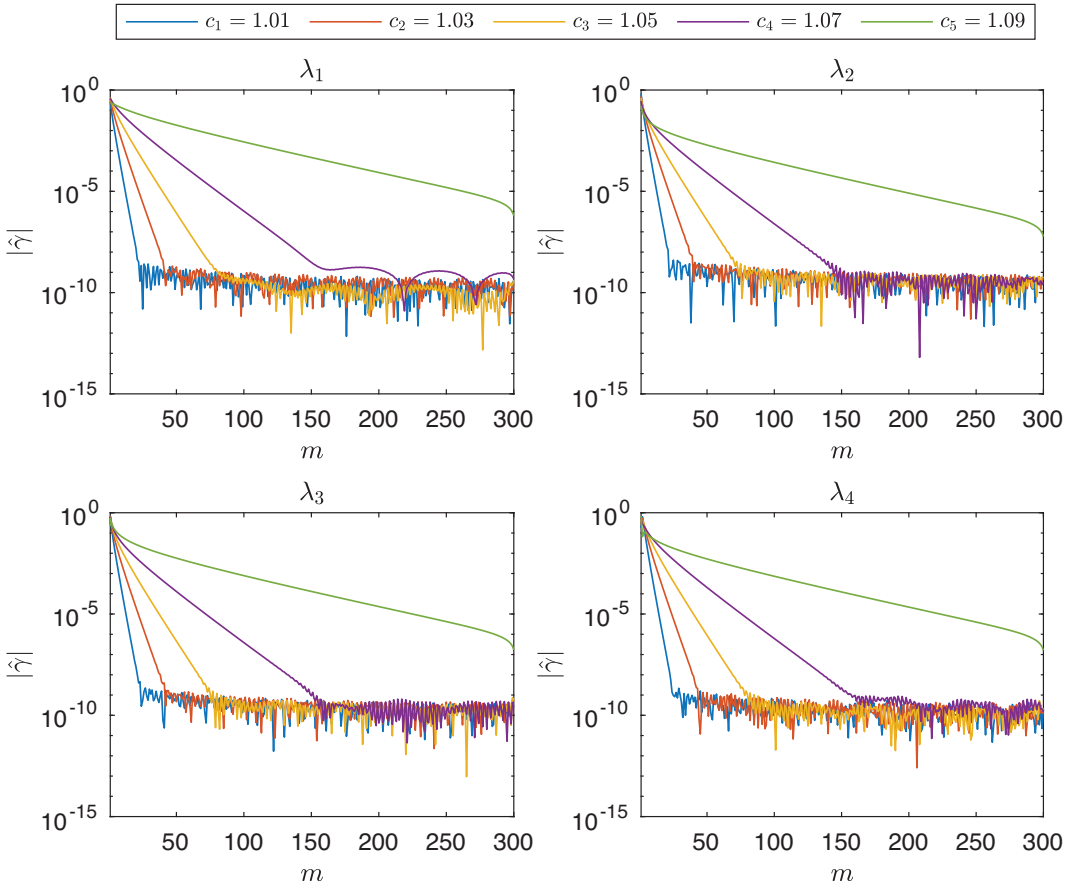


**Figure 4.** The absolute value of eigenfunctions corresponding to the first four eigenvalues in Fourier space is plotted versus  $m \in \{1, \dots, N\}$  for five values of  $c$  in  $(1, c_*)$ . The grid in physical space is chosen to be  $N=300$ , and the solution profiles  $\hat{\eta}$  are obtained from equations (8.4) and (8.5).

To compute eigenvalues for the limiting wave with the peaked profile  $\eta_*$  at  $c = c_*$  in the finite-difference method, we use

$$c = c_* : \quad \mathcal{W}^0(\eta_j) = -\frac{1}{2} - \pi(\delta_0)_j.$$

The Dirac delta distribution is approximated by the Gaussian pulse with a small parameter  $\alpha = \pi/N$  as

$$\delta_0(x) \approx \frac{1}{\sqrt{\pi\alpha^2}} e^{-x^2/\alpha^2}, \quad x \in \mathbb{T}.$$

As is shown in the left panel of figure 5, eigenvalues do not converge well as  $c \rightarrow c_*$  to the limiting eigenvalues at  $c = c_*$  for the fixed value of  $N=300$ .

To illustrate further the low convergence of eigenvalues as  $c \rightarrow c_*$ , we plot the dependence of the third eigenvalue (which is theoretically zero, see [36]) versus  $c$  in figure 6 (left). For computations with different methods and for different  $N$ , we observe the growth  $|\lambda_3|$ , which is a numerical way to detect

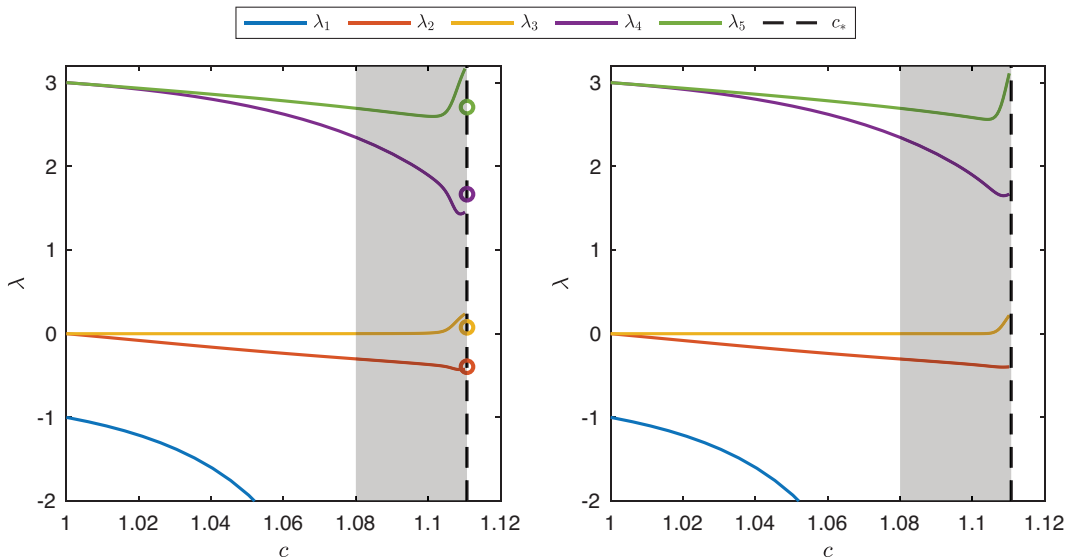


**Figure 5.** The dependence of the first four eigenvalues of the spectral problem (8.7) is plotted versus  $c$  for  $c \in (1, c_*)$  obtained with the finite-difference method (left) and with the Fourier collocation method (right). Eigenvalues computed for the peaked profile with  $c = c_*$  in the finite-difference method (left) are marked as circles. The grid in physical space is chosen to be  $N = 300$ .

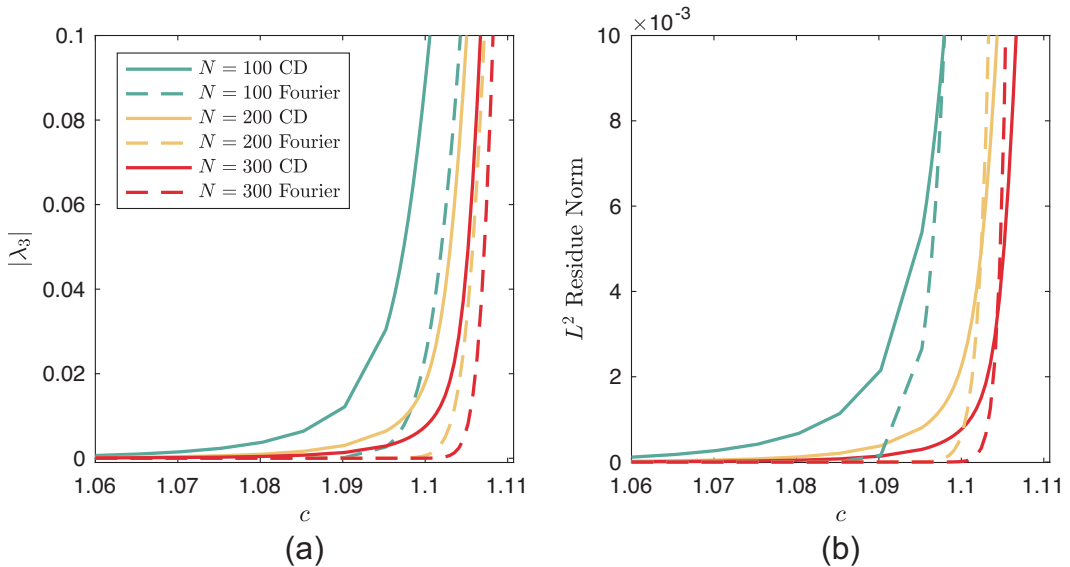


**Figure 6.** (a) The third eigenvalue  $|\lambda_3|$  plotted versus  $c$  to show its departure from 0 as  $c \rightarrow c_*$  for different grids  $N = 100, 200, 300$  by the finite difference (CD) and Fourier collocations (Fourier) methods. (b) The same plots but for the  $L^2$ -norm of the residual terms  $\|\mathcal{L}\gamma_3 - \lambda_3\gamma_3\|_{L^2}$  and  $\|\hat{\mathcal{L}}\hat{\gamma}_3 - \lambda_3\hat{\gamma}_3\|_{L^2}$ .



the loss of accuracy of numerical computations. Similarly, we show in figure 6 (right) the  $L^2$  norms of the residual terms

$$\begin{cases} \|\mathcal{L}\gamma_3 - \lambda_3\gamma_3\|_{L^2} = \left( \sum_{j=-N}^{N-1} |\mathcal{L}\gamma_3(x_j) - \lambda_3\gamma_3(x_j)|^2 \Delta x \right)^{1/2}, \\ \|\widehat{\mathcal{L}}\hat{\gamma}_3 - \lambda_3\hat{\gamma}_3\|_{L^2} = \left( \sum_{k=-N}^N |\widehat{\mathcal{L}}\hat{\gamma}_3(m_k) - \lambda_3\hat{\gamma}_3(m_k)|^2 \Delta m \right)^{1/2}. \end{cases}$$

The residual terms grow as  $c \rightarrow c_*$  in agreement with other figures, and the growth becomes visible for larger values of  $c$  if the truncation number  $N$  is increased.

We conclude that the spectral stability problem for the travelling wave with the peaked profile  $\eta_* \in C_{\text{per}}^0(\mathbb{T}) \cap W^{1,\infty}(\mathbb{T})$  cannot be analysed by working with the spectral stability problem for the family of travelling waves with the smooth profiles  $\eta \in C_{\text{per}}^\infty(\mathbb{T})$  in the limit  $c \rightarrow c_*$ . The lack of convergence is fundamental, both at the levels of functional analysis and numerical approximations. On the analysis side, the linearised system (4.1) for the smooth waves is invalid for the peaked waves and needs to be replaced by the linearised system (4.7). On the numerics side, the eigenvalues of the Hessian operator  $\mathcal{L}$  do not converge well as  $c \rightarrow c_*$  to the limiting eigenvalues at  $c = c_*$  for the fixed value of  $N$ . Due to the lack of convergence, we have a striking discrepancy between the spectral stability of the smooth waves [36] and the spectral instability (theorem 3) of the peaked waves.

## References

- [1] Alber M, Camassa R, Fedorov YN, Holm DD and Marsden JE (1999) On billiard solutions of nonlinear PDEs *Phys. Lett. A* **264**, 171–178.
- [2] Alber M, Camassa R, Holm DD and Marsden JE (1995) On the link between umbilic geodesics and soliton solutions of nonlinear PDEs *Proc. Roy. Soc. London A* **450**, 677–692.
- [3] Amick CJ, Fraenkel LE and Toland JF (1982) On the Stokes conjecture for the wave of extreme form *Acta Math.* **148**, 193–214.
- [4] B  hler T and Salamon DA (2018) *Functional Analysis (Graduate Studies in Mathematics)*, **191**. Providence, RI: AMS.
- [5] Babenko KI (1987) Some remarks on the theory of surface waves of finite amplitude *Sov. Math. Dokl.* **35**, 599–603.
- [6] Bruell G and Dhara RN (2021) Waves of maximal height for a class of nonlocal equations with homogeneous symbols *Indiana Univ. Math. J.* **70**, 711–742.
- [7] Carter JD (2024) Instability of near-extreme solutions to the Whitham equation *Stud. Appl. Math.* **152**, 903–915.
- [8] Chen RM, Di H and Liu Y (2023) Stability of peaked solitary waves for a class of cubic quasilinear shallow-water equations *Int. Math. Res. Not.* **2023**, 6186–6218.
- [9] Chen RM, Lian W, Wang D and Xu R (2021) A rigidity property for the Novikov equation and the asymptotic stability of peakons *Arch. Ration. Mech. Anal.* **241**, 497–533.
- [10] Chen RM and Pelinovsky DE (2021)  $W^{1,\infty}$ -instability of  $H^1$ -stable peakons in the Novikov equation *Dynamics of PDE* **18**, 173–197.
- [11] Constantin A and Molinet L (2001) Orbital stability of solitary waves for a shallow water equation *Physica D* **157**, 75–89.
- [12] Constantin A and Strauss WA (2000) Stability of peakons *Comm. Pure Appl. Math.* **53**, 603–610.
- [13] Constantin A and Strauss WA (2002) Stability of the Camassa–Holm solitons *J. Nonlinear Sci.* **12**, 415–422.
- [14] Deconinck B, Dyachenko SA, Lushnikov PM and Semenova A (2023) The dominant instability of near extreme Stokes waves *Proc. Natl Acad. Sci.* **120**, e2308935.
- [15] Dyachenko SA and Semenova A (2023) Quasiperiodic perturbations of Stokes waves: Secondary bifurcations and stability *J. Comput. Physics* **492**, 112411.
- [16] Dyachenko SA and Semenova A (2023) Canonical conformal variables based method for stability of Stokes waves *Stud. Appl. Math.* **150**, 705–715.
- [17] Ehrman B and Johnson MA (2024) Orbital stability of periodic traveling waves in the  $b$ -Camassa–Holm equation *Phys. D* **461**, 134105.
- [18] Ehrman B, Johnson MA and Lafortune S (2024) Orbital stability of smooth solitary waves for the Novikov equation *J. Nonlinear Sci.* **34**, 116.
- [19] Geyer A, Martins RH, Natali F and Pelinovsky DE (2022) Stability of smooth periodic traveling waves in the Camassa–Holm equation *Stud. Appl. Math.* **148**, 27–61.

- [20] **Geyer A and Pelinovsky DE** (2017) Spectral stability of periodic waves in the generalized reduced Ostrovsky equation *Lett. Math. Phys.* **107**, 1293–1314.
- [21] **Geyer A and Pelinovsky DE** (2019) Linear instability and uniqueness of the peaked periodic wave in the reduced Ostrovsky equation *SIAM J. Math. Anal.* **51**, 1188–1208.
- [22] **Geyer A and Pelinovsky DE** (2020) Spectral instability of the peaked periodic wave in the reduced Ostrovsky equation *Proc. AMS* **148**, 5109–5125.
- [23] **Hakkaev S, Stanislavova M and Stefanov A** (2017) Spectral stability for classical periodic waves of the Ostrovsky and short pulse models *Stud. Appl. Math.* **139**, 405–433.
- [24] **Hakkaev S, Stanislavova M and Stefanov A** (2017) Periodic travelling waves of the regularized short pulse and Ostrovsky equations: Existence and stability *SIAM J. Math. Anal.* **49**, 674–698.
- [25] **Hone ANW, Novikov V and Wang JP** (2018) Generalizations of the short pulse equation *Lett. Math. Phys.* **108**, 927–947.
- [26] **Hunter JK and Saxton R** (1991) Dynamics of director fields *SIAM J. Appl. Math.* **51**, 1498–1521.
- [27] **Johnson ER and Pelinovsky DE** (2016) Orbital stability of periodic waves in the class of reduced Ostrovsky equations *J. Diff. Eqs.* **261**, 3268–3304.
- [28] **Korotkevich AO, Lushnikov PM, Semenova A and Dyachenko SA** (2023) Superharmonic instability of Stokes waves *Stud. Appl. Math.* **150**, 119–134.
- [29] **Lafortune S** (2024) Spectral and linear stability of peakons in the Novikov equation *Stud. Appl. Math.* **152**, 1404–1424.
- [30] **Lafortune S and Pelinovsky DE** (2022) Spectral instability of peakons in the  $b$ -family of the Camassa–Holm equations *SIAM J. Math. Anal.* **54**, 4572–4590.
- [31] **Lafortune S and Pelinovsky DE** (2022) Stability of smooth solitary waves in the  $b$ -Camassa–Holm equations *Physica D* **440**, 133477.
- [32] **Lenells J** (2004) Stability of periodic peakons *Int. Math. Res. Not.* **2004**, 485–499.
- [33] **Lenells J** (2004) A variational approach to the stability of periodic peakons *J. Nonlinear Math. Phys.* **11**, 151–163.
- [34] **Lenells J** (2005) Traveling wave solutions of the Camassa–Holm equation *J. Diff. Eqs.* **217**, 393–430.
- [35] **Lenells J** (2005) Stability for the periodic Camassa–Holm equation *Math Scand.* **97**, 188–200.
- [36] **Locke S and Pelinovsky DE** (2025) On smooth and peaked traveling waves in a local model for shallow water waves *J. Fluid Mech.* **1004**, A1.
- [37] **Locke S and Pelinovsky DE** (2025) Peaked Stokes waves as solutions of Babenko’s equation *Appl. Math. Lett.* **161**, 109359.
- [38] **Long T and Liu C** (2023) Orbital stability of smooth solitary waves for the  $b$ -family of Camassa–Holm equations *Physica D* **446**, 133680.
- [39] **Madiyeva A and Pelinovsky DE** (2021) Growth of perturbations to the peaked periodic waves in the Camassa–Holm equation *SIAM J. Math. Anal.* **53**, 3016–3039.
- [40] **Matsumo Y** (2020) Parametric solutions of the generalized short pulse equations *J. Phys. A: Math. Theor.* **53**, 105202.
- [41] **Natali F and Pelinovsky DE** (2020) Instability of  $H^1$ -stable peakons in the Camassa–Holm equation *J. Diff. Eqs.* **268**, 7342–7363.
- [42] **Plotnikov P** (2002) A proof of the Stokes conjecture in the theory of surface waves *Stud. Appl. Math.* **108**, 217–244.
- [43] **Stanislavova M and Stefanov A** (2016) On the spectral problem  $Lu = \lambda u'$  and applications *Comm. Math. Phys.* **343**, 361–391.
- [44] **Toland JF** (1978) On the existence of a wave of greatest height and Stokes’s conjecture *Proc. R. Soc. Lond. A* **363**, 469–485.
- [45] **Ye W and Yin Z** (2020) Global existence for the periodic dispersive Hunter–Saxton equation *Monats. Math.* **191**, 267–278.